Comprehensive Study on Electrical and Hydrogen Gas Sensing Characteristics of Pt/ZnO Nanocrystalline Thin Film-Based Schottky Diodes Grown on N-Si Substrate Using RF Sputtering

Lintu Rajan, C. Periasamy, and Vineet Sahula, *Senior Member, IEEE*

***Abstract*—This paper presents a comprehensive study on the electrical characteristics of Pt/ZnO thin film Schottky contacts fabricated on n-Si substrates by RF sputtering, and its application as a Hydrogen sensor. The basic structural, surface morphological, and optical properties of the ZnO thin film were also been explored. Pt/ZnO thin film junction was characterized using current–voltage *(I–V)* and capacitance–voltage *(C–V)* measurements at room temperature, exhibiting rectifying behavior with barrier height, ideality factor and series resistance of 0.71 eV *(I–V)*/0.996 eV*(C–V),* 2.5 and ∼95 Ω respectively. The lack of congruence between the values of Schottky barrier heights calculated from *I–V* and *C–V* measurements is interpreted. Cheung's method and modified Norde's functions were employed along with the conventional thermionic emission model, to incorporate the impact of series resistance in the calculation of diode parameters. We unveiled, the Hydrogen sensing characteristics displayed by the Pt/ZnO thin film-based sensor to different concentrations (200–1000 ppm) of Hydrogen at 350 °C. The sensor has exhibited good recoverable transient characteristics under a series of Hydrogen exposure cycles with a maximum sensitivity of 57% at 1000 ppm of Hydrogen.**

***Index Terms*—Electrical characteristics, hydrogen sensing, metal-semiconductor interface, schottky diode, zinc oxide (ZnO) thin film.**

I. Introduction

INC Oxide have garnered widespread attention for the use in diverse applications such as gas sensors, lasers, solar cells, photo detectors, photo catalysts etc, owing to its distinctive properties such as good chemical and thermal stability, wide band gap (3.3 eV), high exciton binding energy (60 meV), high mobility of conducting electrons etc [1]–[6]. ZnO can form excellent Schottky or rectifying contact with high work function noble metals like Pt, Au and Pd and it is the one of the remarkable property due to which ZnO has attracted much research interest among solid state electronic researchers [1]–[10]. The rapid progress of ZnO devices like diodes, sensors, detectors, etc demand the proper understanding and controllability of its metal contacts.

Metal Schottky contact on ZnO was first studied by Mead and Neville [1]. Tsiarapas *et al.* and Yadav *et al.* investigated the Pd Schottky contact on ZnO and reported an ideality factor of ∼1.21 and ∼1.5 respectively [2], [3]. Aydogan *et al.* reported the electrical characterization of Au/n-ZnO Schottky contacts on n-Si using electro deposition technique with an ideality factor of ∼1.21 [4]. Periasamy and Chakrabarti also studied Pt contact on ZnO thin film using vacuum coating technique with an ideality factor of 1.52 [5]. Li *et al.* and Lp *et al.* reported the fabrication of Pt Schottky contacts on ZnO using pulse laser deposition with an ideality factor of ∼2.96 and ∼1.7 respectively [8], [11]. However, there is no significant report on fabrication and characterization of RF Sputtered Pt/ZnO Schottky contact on n-Si substrate for gas sensing applications.

Hydrogen has got heightened focus due to its importance in the present context where the shift to greener source of energy is highly demanding and Hydrogen can act as an alternative to fossil fuels. Extensive research in Hydrogen sensing is highly recommended as it is a colorless, odorless and highly inflammable gas which can spontaneously ignite with Oxygen forming potentially explosive mixtures [10]–[13]. Majority of commercial gas sensors are based on thin/thick layers or nanostructure-based metal oxide semiconductors, such as SnO_2,TiO_2, Fe_2O_3, ZnO, etc., integrated with heaters to raise the temperature to the achieve the optimum performance. ZnO nanostructure-based gas sensors simulated an exciting interest recently, due to their notable advantages, such as high surface to volume ratio, easy to fabricate structure, good chemical and thermal stability, better response, etc., [14]–[16]. Nanocrystalline thin films are having the additional advantage of reproducibility of film quality and ease of deposition. Also, it was reported that thin films possess better recovery characteristics compared to other configurations [17]. Noble metals like Pt, Pd and Au are considered to be important catalysts for Hydrogen sensing reactions [10].

We have investigated the Hydrogen sensing characteristics of Pt/ZnO thin film in this study. To the best of our knowledge, the proposed sensor structure, based on ZnO thin film with Pt catalytic dots on the surface, having the advantage of simple and easy to fabricate structure and devoid of any additional electrical contacts other than Pt catalytic contacts on the surface has not yet reported. We have discussed the trends in sensor performance and have tried to give an adequate explanation for

Manuscript received May 25, 2015; revised September 15, 2015 and December 17, 2015; accepted December 18, 2015. Date of publication; date of current version. This work was supported by CeNSE, Indian Institute of Science, Bangalore, where the part of the reported work (fabrication/characterization) was carried out under INUP which have been sponsored by DIT, MCIT, Government of India. The review of this paper was arranged by Associate Editor Z. Zhong.

The authors are with the Malaviya National Institute of Technology, Jaipur 302017, India (e-mail: linturajan08@gmail.com; cpsamy.ece@mnit.ac.in; vsahula.ece@mnit.ac.in).

Color versions of one or more of the figures in this paper are available online at http://ieeexplore.ieee.org.

Digital Object Identifier 10.1109/TNANO.2015.2513102

these trends. We have also discussed the basic microstructure study and optical properties of RF sputtered ZnO thin film.

II. Experimental Details

A. ZnO Thin Film Fabrication

ZnO thin film was deposited on the n-Si substrate (Resistivity of 1–10 Ω) by RF sputtering system equipped with high purity ZnO (99.99%) target. Before loading into the sputtering system, Si substrate of thickness 425 μm was organically and ionically cleaned using standard RCA process. The substrate was loaded into a magnetron sputtering system with a target to substrate distance fixed at 11 cm. Mechanical rotary and turbo pump were used to evacuate the sputtering chamber to the pressure of 1.5×10^{-6} Torr, before generation of plasma activated by RF power of 100 W. Sputtering gas used was Argon (99.999% pure) and its concentration was kept at 15 SCCM (standard cubic centimeter per minute) using the mass flow controller (MFC). To remove the impurities on ZnO target, it was pre-sputtered for 10 min before deposition. ZnO thin film was sputter deposited on substrates at the pressure of 1.8×10^{-2} Torr for 40 min. After deposition, rapid thermal annealing was performed at 450 °C for 10 min to improve the crystallinity of the film. The film thickness was measured by the surface profiler and was around 200 nm.

B. ZnO Thin Film Characterization

The crystalline properties of ZnO thin film were characterized by X-ray diffraction (XRD) using 18 kW Cu rotating-anode-based X-ray diffractometer (Panalytical X Pert Pro) with Cu Kα as the line source ($\lambda = 1.542$ Å). A Field emission scanning electron microscope (Nova Nano FE-SEM, 450) and Energy Dispersive X-ray (EDX) Spectroscopy (EDS-INCA, Oxford Instruments, UK) were used to investigate the surface morphologies and elemental compositions of the thin film respectively. Photoluminescence (PL) measurements at room temperatures were carried out using fluorescence spectrometer (Perkin Elmer, LS55) which uses a He–Cd laser of 325 nm emission line. Optical transmittance and absorbance of the film was measured using UV/VIS/NIS spectrometer (Perkin Elmer, Lambda 750), which uses deuterium and tungsten halogen light sources. All measurements were carried out at room temperature.

C. Device Fabrication and Characterization

To study the electrical properties and gas sensing behavior of ZnO thin film with Pt catalytic dots, an array of Pt Schottky contacts each of area 3.8×10^{-3} cm^2 and thickness 80 nm was fabricated on ZnO/n-Si substrate using RF sputtering through shadow mask technique. An 80 nm thick Al layer was also deposited on the back side of n-Si substrate by e-beam evaporation to obtain the ohmic contact. The fabricated device was then undergone rapid thermal annealing at 450 °C for 5 min to realize good electrical conductivity and better contact quality. The Fig. 1(a) shows the FE-SEM image (Top view) of Pt Schottky contacts arrays fabricated on the ZnO thin film, whereas the EDX spectrum is shown in Fig. 1(b). EDX spectrum exhibits an Oxygen peak at energy about 0.52 keV, two Zn peaks at 1.012 and 8.63 keV and two Pt peaks at 9.44 and 2.048 keV, confirming the presence of O, Zn and Pt elements respectively in our sample. The inset of Fig. 1(b) shows the elemental mapping of ZnO and Pt Schottky contacts in the sample. $I - V$ and $C - V$ measurements were obtained using Agilent B1500A semiconductor device analyzer. The gas sensing characteristics were obtained using a computer controlled gas sensing set up comprises of a static mixer, MFC, Keithley-237 source measure unit, a heater made of halogen bulb covered by graphite and a data acquisition system. The device was introduced to several gas exposure cycles of target gas of different concentrations and synthetic air at 350 °C.

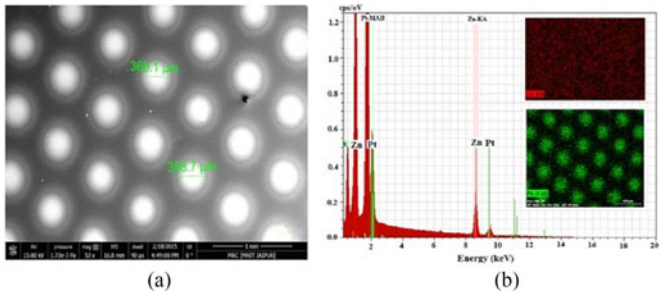

Fig. 1. (a) FE-SEM image of Pt Schottky contacts grown on ZnO thin film. (b) EDX spectra of Pt/ZnO Schottky diodes, the inset shows the mapping data of ZnO (red) and Pt dots (green).

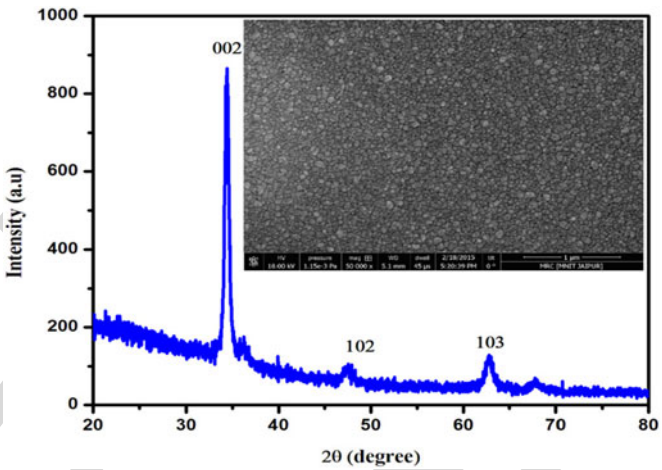

Fig. 2. The XRD pattern of ZnO thin film grown on Si substrate. Inset shows FE-SEM image of ZnO thin film.

III. Results and Discussions

A. Structural and Optical Properties of ZnO Thin Film

In Fig. 2 we present the XRD spectrum for the RF sputtered ZnO thin film on the silicon substrate in the range of 2θ from 20° to 80°. It is having highest peak of [002] appears at around $2\theta = 34.33°$ which is near to that of reference strain free ZnO film peak (34.421°) indicating good crystal quality of film with reduced stress. This also confirms that the film is preferentially C-axis oriented with hexagonal wurtzite structure. The Crystalline size (D) of ZnO thin film is calculated using the Scherrer formula from the full width at half maximum for the prominent

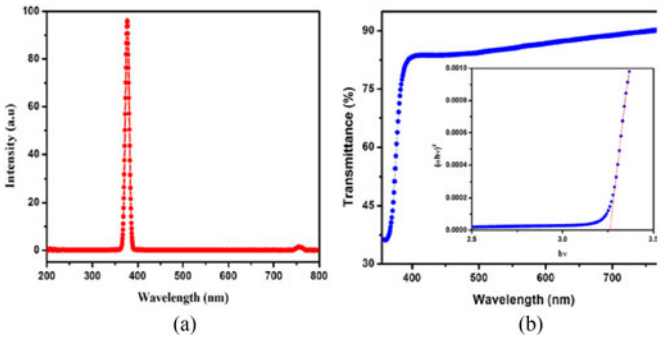

Fig. 3. (a) Room-temperature PL spectra of ZnO thin film on Si substrate. (b) Optical transmittance spectra of ZnO thin film as a function of wavelength. Inset shows the $(\alpha h\upsilon)^2$ versus $h\upsilon$ plot of ZnO thin film for band gap calculation.

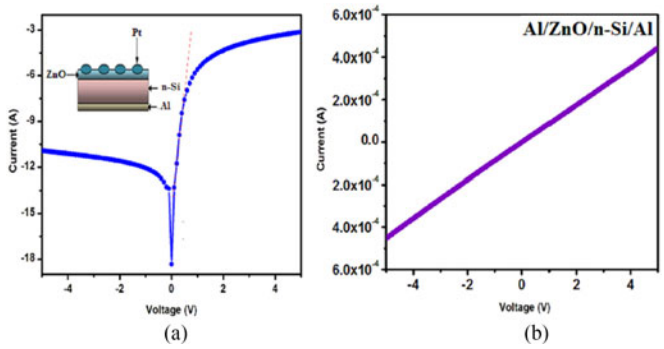

Fig. 4. (a) In *I–V* characteristic for Pt/ZnO thin film interface (dashed line represents linear fit). The inset shows *I–V* measurement set up. (b) The ohmic *I–V* characteristic of Al/n-ZnO/n-Si/Al junction.

(002) peak [18] and is around 18 nm. The lattice constant c and interplanar spacing d are evaluated to be 0.52033 and 0.2602 nm respectively. These values are in good accordance with the experimental results published by others [18], [19]. Inset of Fig. 2 depicts the FE-SEM image of the nanocrystalline ZnO thin film grown on n-Si substrate, which demonstrates that nanostructure grains are uniformly distributed having diameter of about 20 nm.

The PL characteristics of the ZnO thin films were procured in the wavelength range of 200–800 nm at room temperature and is depicted in Fig. 3(a). The film shows a strong UV emission peak at 375 nm which is known as near band edge emission, and it is attributed to the free exciton recombination. The absence of other major peaks, except UV emission confirms high crystallinity of the deposited ZnO thin films with fewer surface defects such as Oxygen vacancies [20]. The band gap of ZnO thin film is obtained as 3.28 eV from PL spectra.

The optical transmittance and absorbance of the film were measured by UV-Visible spectrometer in the range of 200–800 nm. Transmission spectra depicted in the Fig. 3(b) shows good optical transmission in the visible wavelength region (380–780 nm), confirming that sputtered ZnO thin film is transparent in the visible wavelength range. The optical band gap, for the film can be obtained by extrapolating the linear portions of $(\alpha h\upsilon)^2$ versus $h\upsilon$ to $\alpha h\upsilon = 0$, which is illustrated in the inset of Fig. 3(b) and its value is obtained as 3.26 eV [18]–[20].

B. I–V Characteristics of Pt/ZnO Thin Film Schottky Diode

The Pt/ZnO thin film Schottky diodes were electrically characterized using Agilent B1500A semiconductor device analyzer under dark condition. The fabricated Pt/ZnO/n-Si/Al structure is schematically represented in the inset of Fig. 4(a); whereas Fig. 4(a) shows the In *I–V* characteristics of the structure, which confirms the formation of Schottky junction at the Pt/ZnO interface having rectifying ratio I_F/I_R of 637 at ± 1 V. Since the Al/n-ZnO/Si/Al junction shows ohmic behavior as depicted in Fig. 4(b), the proposed structure behaves as vertical Pt/ZnO Schottky diode similar to structures reported by authors in [2]–[4], [21], [22]. We have measured *I–V* characteristics of about five Schottky diodes in the array. All of them exhibited the same characteristics. The Schottky diode parameters were extracted using three different techniques such as conventional thermionic emission model, Cheung's method and Norde's method, which are now discussed in detail. In the conventional method of calculation, we have extracted the electronic parameters such as saturation current, barrier height, and ideality factor of Pt/ZnO Schottky diode by assuming thermionic emission as the only carrier transport mechanism. The forward *I–V* characteristics of the Schottky junction is investigated with help of thermionic emission model, in which current for positive bias voltage is given by (1),neglecting the series resistance [21]–[26].

$$I \approx I_0 \left[\exp\left(\frac{qV}{\eta kT}\right) - 1\right] \tag{1}$$

where, I_0 is the saturation current as depicted in (2), q is the electronic charge, V is the applied voltage, η is the ideality factor, k is the Boltzmann constant and T is the temperature.

$$I_0 = AA^*T^2 \exp\left(\frac{-q\phi_b}{kT}\right) \tag{2}$$

where A is the diode area, $A^*(= 32\,\mathrm{cm}^{-2}\,\mathrm{K}^{-2})$ is the Richardson constant, ϕ_b is the effective barrier height at zero bias [1], [3], [5]. We have calculated the slope of low voltage linear region (0.1 V to 0.3 V) of forward bias In *I–V* characteristics and obtained the value of ideality factor as 2.5 at room temperature using (3) [1], [3], [5].

$$\eta = \frac{q}{kT}\frac{dV}{d\ln(I)}. \tag{3}$$

The departure of ideality factor from the ideal value of 1 indicates the existence of different current conduction mechanisms other than thermionic emission in the Schottky junction like tunneling, tunneling-recombination, field emission etc, presence of series resistance and interfacial layer between metal and semiconductor [23], [27]. The saturation current is calculated from the vertical axis intercept of In *I–V* plot and obtained to be 1.5×10^{-8} A. Effective Barrier height of the Schottky junction is calculated to be 0.71 eV using (2).

These values are in good congruence with the results published by other researchers [5], [8]. According to Schottky–Mott theory, the ideal value of the barrier height for Pt/ZnO Schottky contact varies from 1.3 to 1.95 eV which is given by the difference between work function of Pt and electron affinity of ZnO [23]. The non-ideal values of barrier height (0.71 eV)

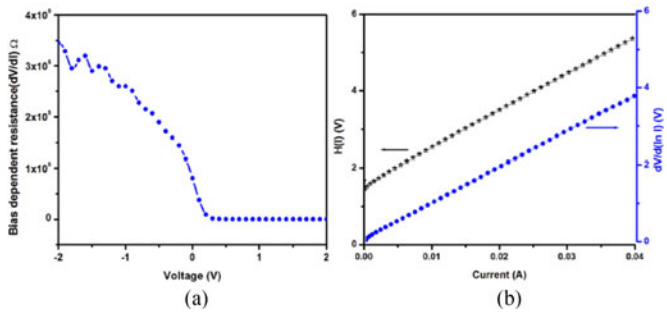

Fig. 5. (a) Bias voltage dependent diode resistance (R_i) of Pt/ZnO interface. (b) Plots of $dv/d(\ln I)$ versus I and $H(I) - I$ of Pt/ZnO thin film diode obtained from experimental *I–V* data in Fig. 4(a).

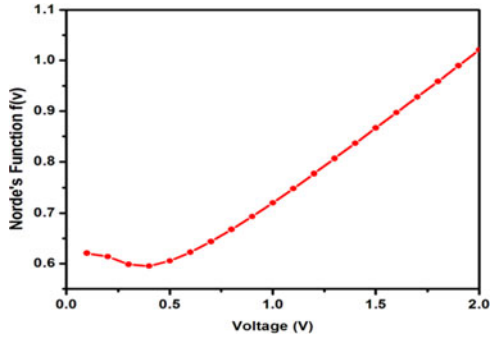

Fig. 6. $F(V)$ versus V plots obtained from the experimental *I–V* data in Fig. 4(a).

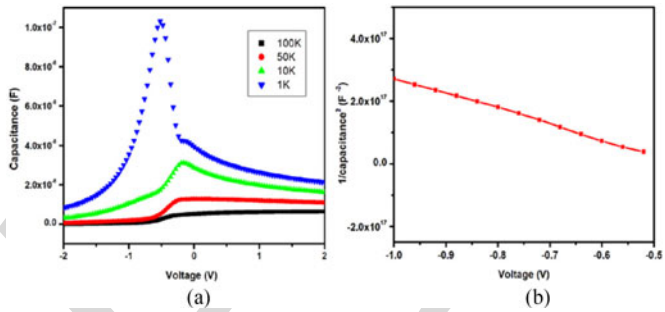

Fig. 7. (a) The frequency dependent *C–V* characteristics of Pt/ZnO Schottky diode. (b) $C^{-2} - V$ characteristics of Pt/ZnO Schottky diode at $f = 50$ KHz.

and ideality factor (2.5) measured from *I–V* characteristic can be credited to the presence of interface states between metal (Pt) electrode and semiconductor (ZnO) surface, Fermi energy level pinning caused by surface states, barrier inhomogeneities and certain other interface specific effects [1], [2], [23], [27].

In order to gain insight regarding the value of series resistance, we studied bias dependent resistance, $R_i (R_i = dV/dI)$ *versus* V plot as shown in Fig. 5(a). It is obvious from the plot that that R_i has got a bias independent constant value of around 95 Ω at higher voltages, and this corresponds to series resistance [22]. To incorporate the effect of series resistance, R_s in our Schottky diode parameter calculations, we have employed the analysis technique reported by Cheung and Cheung [28]. Cheung's functions can be written as:

$$\frac{dV}{d(\ln I)} = \frac{\eta kT}{q} + IR_s \tag{4}$$

$$H(I) = V - \frac{\eta kT}{q} \ln\left(\frac{I}{AA^*T^2}\right) \tag{5}$$

$$H(I) = \eta\phi_b + IR_s. \tag{6}$$

From the slope and vertical axis intercept of $dv/d(\ln I)$ versus I plot displayed in Fig. 5(b), value of series resistance (R_s) and ideality factor η are obtained as 96.2 Ω and 2.34 respectively. In order to determine the value of barrier height, we have also plotted $H(I)$ versus I curve using the value of ideality factor obtained from $dv/d(\ln I)$ versus I plot. Schottky barrier height (ϕ_b) is extracted from the vertical axis intercept of *H(I)* versus *I* plot given in the Fig. 5(b) and is obtained as 0.65 eV, whereas its slope will give the value of series resistance, which is equal to 96.6 Ω. There is a disparity in the Schottky barrier height value obtained from conventional thermionic emission model and Cheung's technique. This is because, Cheung's plots are obtained from the downward curvature region of *I–V* characterization, which strongly suggests the presence of series resistance and insulating interfacial layer across Pt/ZnO Schottky junction, whereas parameters are calculated from low voltage linear region of *I–V* characteristic in thermionic emission model. Furthermore, the closely agreed values of series resistance calculated from both the plots of Fig. 5(b), is a proof for the consistency of Cheung's approach of calculations [2], [4], [28]. An alternative approach developed by Norde is also employed to determine the value of series resistance [29], [30]. The Norde function is described as in (7).

$$F(V) = \frac{V}{\gamma} - \frac{kT}{q} \ln\left(\frac{I(V)}{AA^*T^2}\right) \tag{7}$$

$$\phi_b = F(V_{\min}) + \frac{V_o}{\gamma} - \frac{kT}{q} \tag{8}$$

$$R_s = \frac{kT(\gamma - n)}{qI} \tag{9}$$

where γ is an integer greater than ideality factor (here 3), $I(V)$ is the current obtained from *I–V* curve, $F(V_{\min})$ is the minimum value of $F(V)$ and V_0 is the voltage corresponding to $F(V_{\min})$. Fig. 6 depicts the $F(V)$ versus V curve of the Pt/ZnO thin film Schottky diode. The value of barrier height and series resistance obtained from Norde's technique using (8) and (9) are 62.5 Ω and 0.73 eV respectively. These values are in near accordance with value that obtained from the conventional thermionic emission model and Cheung's method, confirming the accuracy of our calculations.

C. C–V Characteristics of Pt/ZnO Thin Film Schottky Diode

Fig. 7(a) displays the frequency dependence of *C–V* characteristics of Pt/ZnO thin film Schottky diode. The graph illustrates that capacitance decreases with increasing frequency, which is an evidence for the existence of interface states and its progressive decrease of the response to the applied ac voltage [27]. At lower frequencies, the interface states can faith-

fully follow the ac signal resulting in higher capacitance values; whereas at higher frequencies, contribution of interface states to total capacitance is very small resulting in lower capacitance value, since the charge at interface states cannot respond spontaneously to the ac signal, [29]–[31]. The *C–V* characteristics can be studied with the help of reverse bias $C^{-2} - V$ characteristics of the diode depicted in Fig. 7(b). The linear curve confirms that doping concentration N_d is constant throughout the depletion region. Depletion layer capacitance is given by following equations.

$$\frac{1}{C^2} = \frac{2\left(V_{\rm bi} - V - \frac{kT}{q}\right)}{q\varepsilon_s\varepsilon_0 A^2 N_d} \tag{10}$$

$$\frac{d(C^{-2})}{d(V)} = \frac{2}{q\varepsilon_s\varepsilon_0 A^2 N_d} \tag{11}$$

where, $V_{\rm bi}$ is the built-in potential, obtained from the intercept of $C^{-2} - V$ curve, ε_s the dielectric constant of the semiconductor ($9\varepsilon_0$ for ZnO), ε_0 is the dielectric constant of vacuum (8.85×10^{-12} F/m), N_d is the concentration of ionized donors and A is the diode area [27], [29].

Carrier concentration N_d can be determined from the slope of $C^{-2} - V$ curve, using (11) and found to be $1 \times 10^{16}\,{\rm cm}^{-3}$. The barrier height of Pt/ZnOSchottky contact can be obtained from *C–V* measurements using (12).

$$\phi_b = q\left[V_{\rm bi} + \frac{kT}{q}\ln\frac{N_c}{N_d}\right] \tag{12}$$

where, N_c is the density of states in the conduction band and its value is $3.5 \times 10^{18}\,{\rm cm}^{-3}$ for ZnO at room temperature [22]. The barrier height of Pt/ZnO thin film Schottky diode is determined as 0.996 eV from the *C–V* measurement which is larger than the barrier heights obtained from the *I–V* measurements. This barrier height variation is possibly due to the effect of lowering of barrier energy induced by image force for (Schottky effect), barrier in-homogeneities caused by intrinsic and extrinsic factors such as grain boundaries, defects, etc., metal induced gap states and presence of an unavoidable interface layer between metal and semiconductor surface [26].

The density of interface states, $N_{\rm ss}$ was calculated using *I–V* and *C–V* characteristics using (13) [22], [28]–[30].

$$N_{\rm ss} = \frac{1}{q}\left[\frac{\varepsilon_i}{\delta}\{n(V) - 1\} - \frac{\varepsilon_s}{W_D}\right] \tag{13}$$

where, ε_i is the permittivity of interface layer, δ is the interface layer thickness, $n(V)$ is the voltage dependent ideality factor and W_D is the width of depletion layer which was obtained from *C–V* characteristics. The value of $N_{\rm ss}$ was obtained to be around $2.03 \times 10^{15}\,{\rm eV}^{-1}{\rm cm}^{-2}$ at 0.5 V.

D. Gas Sensing Properties of Pt/ZnO Thin film

In the proposed sensor structure, the sensor element, i.e., nanocrystalline ZnO thin film is provided with Pt catalytic dots or Schottky contacts on the surface. We represent the *I–V* characteristics of the sensor at different Hydrogen concentrations and air in Fig. 8, whereas its inset provides the schematic structure of the sensor. We have also studied the Hydrogen sensing

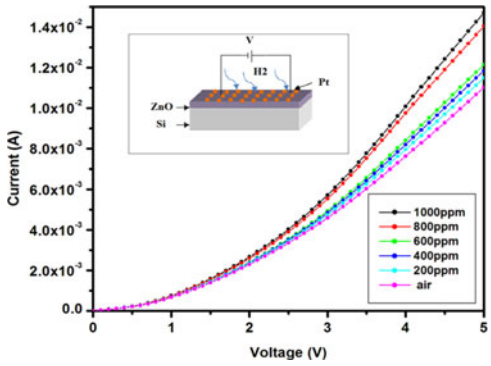

Fig. 8. *I–V* characteristics of the sensor at different Hydrogen concentrations at 350 °C., Inset shows schematic structure of proposed sensor.

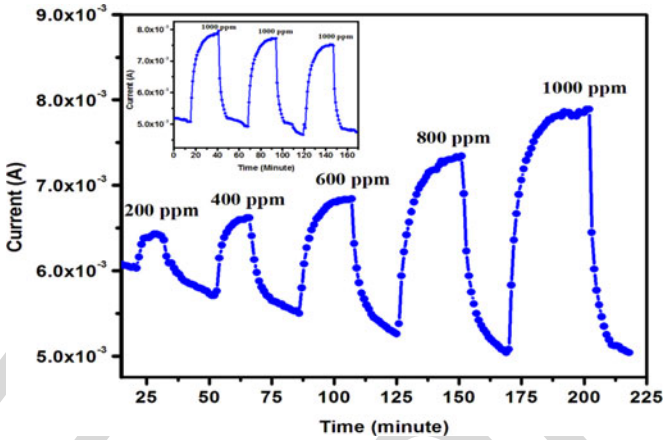

Fig. 9. Dynamic characteristic of the device at different concentrations of Hydrogen at 350 °C. Inset shows repeatability of device at 1000 ppm Hydrogen and 350 °C.

capability of the device by monitoring the current change caused by the adsorption and desorption of target gas (H_2) at 200 ppm-1000 ppm of Hydrogen at 350 °C. which is represented in Fig. 9 and its inset elucidate the repeatability of device at the 1000 ppm Hydrogen. The Sensitivity of the device, *S* was defined as the relative variation of the current in the presence and absence of Hydrogen and is given by (14) [25], [26].

$$S(\%) = \left\{\frac{I_{H_2} - I_{\rm air}}{I_{\rm air}}\right\} \times 100 \tag{14}$$

where, $I_{\rm air}$ is sensor current in the presence of air and I_{H2} is the sensor current after exposing to H_2 gas. The sensitivity has been calculated using (14), and it is noted that sensitivity is directly proportional to Hydrogen concentration, having values of 6.46%, 15.7%, 23.9%, 39.8% and 57% at Hydrogen concentrations of 200 ppm, 400, 600, 800 and 1000 ppm respectively. We have observed a considerable drift in the baseline current of the sensor at different concentrations, which is explained in the later section. Response time of our sample is calculated as the time required for the sensor current to reach 90% of the saturation value in the presence of Hydrogen whereas recovery time is defined as the time required for the sensor current to return to 10% of its baseline value in the presence of synthetic air. It would be worth noting that, while response time increases with increase

TABLE I
ELECTRICAL AND GAS SENSING PARAMETERS OF PT/ZNO THIN FILM SCHOTTKY DIODE

A	Electrical characteristics of Pt/ZnO thin film Schottky diode			
		Cheung's method		
Parameters	Conventional *I-V* method	dV/dlnI versus I	H(I) versus I	Norde's method
Ideality factor	2.5	2.34	–	–
Barrier height (eV)	0.71	0.65	–	0.73
Series resistance (Ω)	∼95	96.2	96.6	62.5

B	Gas sensing characteristics of Pt/ZnO thin film Schottky diode				
	Concentration of Hydrogen				
Parameter	200	400	600	800	1000
Sensitivity (%)	6.46	15.7	23.9	39.8	57
Response(min)	2	5	6	11	15
Recovery(min)	2	4	4	3.5	3.5

in Hydrogen concentration, there is no significant change in recovery time as the target gas concentration increases. It is interesting to note that, in this study recovery time is less than the response time, and similar to observation as reported by Hassan *et al.* [26]. All the sensing parameters obtained from are listed in Table I. We have analyzed the possible reasons for the various trends observed in sensor performance and proposed justification for these trends in the following section.

A brief review on previously reported literature on the Hydrogen sensing characteristics of ZnO, incorporating Pt as the catalyst has been provided in Table II [17], [32]–[34]

E. Hydrogen Sensing Mechanism of Pt/ZnO Thin Film

The change in electrical conductivity of the sensor element upon introduction and removal of target gas can be explained as follows: when Pt/ZnO thin film junction is exposed to synthetic air, Oxygen molecules will get chemisorbed on ZnO surface, forming Oxygen ions by extracting electrons from the conduction band of ZnO. This will create a depletion region in the ZnO surface, causing high electrostatic potential across Pt/ZnO Schottky interface and decreasing the electrical conductivity of ZnO surface. The Pt dots on ZnO thin film can enhance the Oxygen spill over process, by providing a lower energy path for the gaseous species be adsorbed on the metal surface and then diffuse to the ZnO surface [35], [36]. This can result in a large amount of chemisorbed Oxygen. Oxygen chemisorptions reactions are represented as $\mathrm{O}_{2(\mathrm{gas})+}e- \rightarrow \mathrm{O}^{-}_{2(\mathrm{ads}),}\mathrm{O}^{-}_{2(\mathrm{ads})} + \mathrm{e} \rightarrow 2\mathrm{O}^{-}_{(\mathrm{ads}),}2\mathrm{O}^{-}_{(\mathrm{ads})} + \mathrm{e} \rightarrow \mathrm{O}^{2^{-}}_{(\mathrm{ads})}$ [24].

It is important to note that noble metals like Pt, Pd and Au on metal oxide surface can act as a catalyst for dissociation of Hydrogen into Hydrogen atoms [10], [37], [38]. The hydrogen atoms then diffuse through the Pt to reach Pt/ZnO interface and the built-in electric field causes the polarization of Hydrogen atoms, resulting in a dipole layer at Pt/ZnO interface, which will lowers the work function of metal and the Schottky barrier height, increasing the current flow [10], [39]. This is obvious from the *I–V* characteristics of the sensor in Fig. 8. The increase in electrical conductivity of sensor element upon exposure to Hydrogen can also be attributed to the surface reaction between dissociated Hydrogen atoms and chemisorbed Oxygen species on ZnO thin film surface and the subsequent release of electrons to the conduction band of ZnO. The chemical reactions involved are reproduced below $4\mathrm{H} + \mathrm{O}_2^- \rightarrow 2\mathrm{H}_2\mathrm{O} + \mathrm{e}^-$, $2\mathrm{H} + \mathrm{O} \rightarrow \mathrm{H}_2\mathrm{O} + \mathrm{e}^-$, $2\mathrm{H} + \mathrm{O}^2 \rightarrow \mathrm{H}_2\mathrm{O} + 2\mathrm{e}^-$ [25], [36].

In transient response curves given in Fig. 9, we observe a major drift in the baseline current value in the repeated exposure cycles of Hydrogen and synthetic air. This can be attributed to the inefficient chemisorptions of Oxygen molecules and incomplete desorption of Hydrogen atoms from ZnO thin film surface upon exposure to synthetic air [26]. It is also reported that noble metals like Pd and Pt undergo volume change upon repeated Hydrogen exposure, causing embrittlement effect and adversely affect the stability of sensor [38], [39]. However, high temperature enhances the desorption rate which is evidenced from the small recovery time. It is clear from Table I, that the response time increases with the increase in concentration of Hydrogen in the subsequent cycles. This can be attributed to the additional hydroxyl and water products formation during Hydrogen adsorption process. This event could also be the reason for the instability of baseline current value [37], [40].

The sensitivity, S as a function of Hydrogen concentration can empirically be expressed as in (15) [24], [41].

$$S = A(C_{(g)})^{\beta} + 1 \tag{15}$$

where *A* and β are empirically obtained parameters depends on the stoichiometry of surface reactions involved in gas sensing, C_g is the target gas concentration. It was reported that β is 0.5, if the adsorbed Oxygen species is O^{2-} and is 1 if the dominant adsorbed species is O^- [24], [35]. The equation in (15) can also be expressed as follows.

$$\log(S_g - 1) = \log A + \beta \log C_{(g)}. \tag{16}$$

The Fig. 10 depicts the plot of $\log(S_g - 1)$ versus $\log C_{\mathrm{g}}$ which is linear according to (16) with a slope of $\beta = 0.95$. The value of β strongly recommends that the dominant adsorbed Oxygen species on the ZnO thin film surface is O^-. It is worth mentioning that doubly negative Oxygen ion (O^{2-}) is more efficient in depleting the ZnO surface and thus enhancing the sensitivity of Pt/ZnOSchottky junction compared to O^- [41].

TABLE II
A BRIEF SUMMARY OF ZNO BASED HYDROGEN SENSORS, INCORPORATING PT AS A CATALYST

Sensing Material	Deposition Technique	Concentration of Hydrogen	Sensing Performance	Ref
Pt-doped ZnO single layer film	Chemical precipitation	0.2%	$\sim$2 (R_{air}/R_{H2}) (330 °C)	[32]
Pt/ZnO Schottky diode	E-Beam Evaporation	5 ppm H_2	Change of 50 mV bias at 8 mA.(298 K)	[33]
Pt/iZnO Schottky diode	CVD	10 000 ppm	Barrier height change = 207.8 mV(350 K)	[34]
Pt-coated ZnO thin film/Nanorod	PLD(thin film), MBE(Nanorod)	500 ppm	Response of nanorod is higher	[17]
ZnO thin film with Pt dots(*Current work*)	RF sputtering	1000 ppm	Relative Response of 57% (350 °C)	–

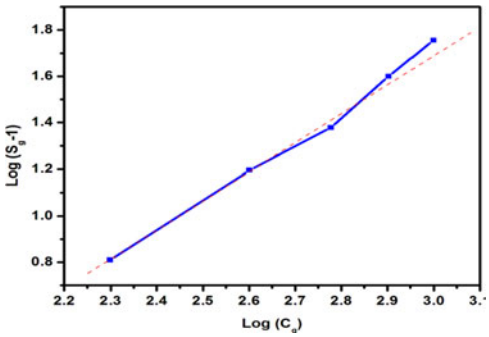

Fig. 10. $\log(S_g - 1)$ versus *log* C_g plot of Pt/ZnO thin film based Hydrogen sensor (dashed line represents the linear fit).

The less abundance of O^- on the Pt/ZnO thin film surface could be a reason for the relatively low sensitivity of the proposed device at the lower concentrations of Hydrogen.

The PL spectra of ZnO thin film elucidated in Fig. 3(a) is devoid of any broad emission peaks except the major emission peak at 380 nm which confirms that the ZnO thin film is highly crystalline with minimum surface defects such as Oxygen vacancies (V_0^{2+}). It is reported that defects such as Oxygen vacancies can enhance the adsorption and desorption process on the ZnO surface by making the nanostructure unstable and increasing the adsorption sites on film surface [24]. Thus, the minimum number of defects on ZnO thin film surface could justify for higher response time of Pt/ZnO thin film surface at higher concentrations.

We have obtained the optimum results at high temperature (350 °C). Many reports have also confirmed this fact that, a nanostructured ZnO-based gas sensors exhibits maximum sensitivity at elevated temperatures usually above 300 °C. This could be attributed to the fact that, Hydrogen atoms can overcome the potential barrier to react with adsorbed Oxygen species only at high temperatures [36], [41]. It is worth mentioning that the factors such as surface to volume ratio, surface defects, quantity of adsorption sites, etc., have significant impact on the surface-controlled reactions involved in gas sensing mechanism of metal oxide semiconductor-based gas sensors. The performance of Pt/ZnO thin film junction can be further improved by optimizing the surface morphology of sensor surface [40]–[42].

IV. CONCLUSION

In this manuscript, we have investigated the electrical and gas sensing characteristics of Pt/ZnOthin film Schottky contacts grown on n-Si substrate by RF sputtering. The structural and optical properties of the ZnO thin film have been characterized by XRD, FE-SEM, EDX, UV and PL spectroscopy, which has confirmed its good crystalline nature. We have estimated characteristic parameters of Pt/ZnOSchottky diode such as barrier height, ideality factor and series resistance, using (*I–V*) and (*C–V*) characterizations being $\sim$0.71 eV $(I - V)/\sim 0.996\,\mathrm{eV}$ (*C–V*), $\sim$2.25 and $\sim$95 Ω respectively at room temperature. An investigation on the gas sensing characteristics of the device towards different concentrations of Hydrogen (200–1000 ppm) at 350 °C revealed a maximum sensitivity of 57% at 1000 ppm Hydrogen. The device has been proposed to be of simple and easy to fabricate structure, having response increasing linearly with Hydrogen concentration.

ACKNOWLEDGMENT

The authors would like to thanks Materials Research Centre, MNIT Jaipur for the fabrication and characterization facility.

REFERENCES

[1] R. C. Neville and C. A. Mead, "Surface barriers on zinc oxide," *J. Appl. Phys.*, vol. 41, no. 9, pp. 3795–3800, 1970.
[2] C. Tsiarapas, D. Girginoudi, and N. Georgoulas, "Electrical characteristics of Pd Schottky contacts on ZnO films," *Mater. Sci. Semicond. Process.*, vol. 17, pp. 199–206, 2014.
[3] A. B. Yadav, A. Pandey, and S. Jit, "Pd Schottky contacts on sol-gel derived ZnO thin films with nearly ideal richardson constant," *IEEE Electron Device Lett.*, vol. 35, no. 7, pp. 729–731, Jul. 2014.
[4] S. Aydogan, K. Cinar, H. Asil, C. Coskun, and A. Turut, "Electrical characterization of Au/n-ZnO Schottky contacts on n-Si," *J. Alloys Compounds*, vol. 476, no. 1, pp. 913–918, 2009.
[5] C. Periasamy and P. Chakrabarti, "Structural and electrical properties of metal contacts on n-type ZnO thin film deposited by vacuum coating technique," *J. Vac. Sci. Technol. B*, vol. 27, no. 5, pp. 2124–2127, Aug. 2009.
[6] J. Iqbal, T. Jan, Y. Ronghai, S. H. Naqvi, and I. Ahmad, "Doping induced tailoring in the morphology, band-gap and ferromagnetic properties of biocompatible ZnO nanowires, nanorods and nanoparticles," *Micro Nano Lett.*, vol. 6, no. 3, pp. 242–251, 2014.
[7] C. Periasamy and P. Chakrabarti, "Time-dependent degradation of Pt/ZnO nanoneedle rectifying contact based piezoelectric nanogenerator," *J. Appl. Phys.*, vol. 109, p. 054306, 2011.
[8] Y. Z. Li, X. M. Li, and X. D. Gao, "Effects of post-annealing on Schottky contacts of Pt/ZnO films toward UV photodetector," *J. Alloys Compounds*, vol. 509, no. 26, pp. 7193–7197, 2011.
[9] Z. Shao, L. Wen, D. Wu, X. Zhang, S. Chang, and S. Qin, "Pt/ZnO Schottky nano-contact for piezoelectric nanogenerator," *Phys. E, Low Dimensional Syst. Nanostruct.*, vol. 43, no. 1, pp. 173–175, 2010.
[10] A. B. Yadav, C. Periasamy, S. Bhaumik, and S. Jit, "Hydrogen gas sensing properties of Pd/ZnO thin films grown on n-Si substrates at room-temperature by thermal evaporation and sol-gel techniques: A comparative study," *Indian J. Pure Appl. Phys.*, vol. 51, no. 11, pp. 792–799, 2013.
[11] K. Ip, Y. W. Heo, K. H. Baik, D. P. Norton, S. J. Pearton, S. Kim, J. R. LaRoche, and F. Ren, "Temperature-dependent characteristics of Pt Schottky contacts on n -type ZnO," *Appl. Phys. Lett.*, vol. 84, no. 15, pp. 2835–2837, 2004.

[12] D. Kohl, "Function and applications of gas sensors," *J. Phys. D, Appl. Phys.*, vol. 34, no. 19, pp. R 125–R 149, 2001.
[13] J. Graetz, "New approaches to hydrogen storage," *Chem. Soc. Rev.*, vol. 38, no. 1, pp. 73–82, 2009.
[14] E. Comini, C. Baratto, I. Concina, and G. Faglia, "Metal oxide nanoscience and nanotechnology for chemical sensors," *Sens. Actuators B, Chem.*, vol. 179, pp. 3–20, 2013.
[15] P. T. Moseley, "Materials selection for semiconductor gas sensors," *Sens. Actuators B, Chem.*, vol. 6, no. 1, pp. 149–156, 1992.
[16] J. Wang, F. Yang, X. Wei, Y. Zhang, and L. Wei, "Controlled growth of conical nickel oxide nanocrystals and their high performance gas sensing devices for ammonia molecule detection," *Phys. Chem. Chem. Phys.*, vol. 16, no. 31, pp. 16711–16718, 2014.
[17] L. C. Tien, P. W. Sadik, D. P. Norton, and L. F. Voss, "Hydrogen sensing at room temperature with Pt-coated ZnO thin films and nanorods," *Appl. Phys. Lett.*, vol. 87, no. 22, p. 222106, 2005.
[18] S. Sharma, S. Vyas, C. Periasamy, and P. Chakrabarti, "Structural and optical characterization of ZnO thin films for optoelectronic device applications by RF sputtering technique," *Superlattices Microstruct.*, vol. 75, pp. 378–389, 2014.
[19] C. Gu, J. Li, J. Lian, and G. Zheng, "Electrochemical synthesis and optical properties of ZnO thin film on In 2 O 3: Sn (ITO)-coated glass," *Appl. Surf. Sci.*, vol. 253, no. 17, pp. 7011–7015, 2007.
[20] P.-T. Hsieh, Y.-C. Chen, C.-M. Wang, Y.-Z. Tsai, and C.-C. Hu, "Structural and photoluminescence characteristics of ZnO films by room temperature sputtering and rapid thermal annealing process," *Appl. Phys. A*, vol. 84, pp. 345–349, 2006.
[21] D. Somvanshi and S. Jit, "Mean barrier height and Richardson constant for Pd/ZnO thin film-based Schottky diodes grown on n-Si substrates by thermal evaporation method," *IEEE Electron. Device Lett.*, vol. 34, no. 10, pp. 1238–1240, Oct. 2013.
[22] D. Somvanshi and S. Jit, "Analysis of I–V characteristics of Pd/ZnO thin film/n-Si schottky diodes with series resistance," *J. Nanoelectron. Optoelectron.*, vol. 9, pp. 21–26, 2014.
[23] I. Hussain, M. Y. Soomro, N. Bano, O. Nur, and M. Willander, "Interface trap characterization and electrical properties of Au-ZnO nanorod Schottky diodes by conductance and capacitance methods," *J. Appl. Phys.*, vol. 112, no. 6, p. 064506, 2012.
[24] Y. Shi, M. Wang, C. Hong, Z. Yang, J. Deng, and X. Song, "Multi-junction joints network self-assembled with converging ZnO nanowires as multi-barrier gas sensor," *Sens. Actuators B, Chem.*, vol. 177, pp. 1027–1034, 2013.
[25] S. Ren, G. Fan, S. Qu, and Q. Wang, "Enhanced H2 sensitivity at room temperature of ZnO nanowires functionalized by Pd nanoparticles," *J. Appl. Phys.*, vol. 110, p. 084312, 2011.
[26] J. J. Hassan, M. A. Mahdi, C. W. Chin, and H. Abu-Hassan, "A high-sensitivity room-temperature hydrogen gas sensor based on oblique and vertical ZnO nanorod arrays," *Sens. Actuators B, Chem.*, vol. 176, pp. 360–367, 2013.
[27] S. M. Sze, *Physics of Semiconductor Devices*, 2nd ed. New York, NY, USA: Wiley, 1981.
[28] S. K. Cheung and N. W. Cheung, "Extraction of Schottky diode parameters from forward current-voltage characteristics," *Appl. Phys. Lett.*, vol. 49, no. 2, pp. 85–87, 1986.
[29] S. Karataş, S. Altındal, A. Türüt, and M. Cakar, "Electrical transport characteristics of Sn/p-Si schottky contacts revealed from I–V–T and C–V–T measurements," *Phys. B, Condens. Matter*, vol. 392, nos. 1/2, pp. 43–50, 2007.
[30] W. G. Osiris, A. A. M. Farag, and I. S. Yahia, "Extraction of the device parameters of Al/P 3 OT/ITO organic Schottky diode using J–V and C–V characteristics," *Synthetic Metals*, vol. 161, no. 11, pp. 1079–1087, 2011.
[31] M. Cakar, N. Yıldırım, H. Doğan, and A. Türüt, "The conductance and capacitance–frequency characteristics of Au/pyronine-B/p-type Si/Al contacts," *Appl. Surf. Sci.*, vol. 253, pp. 3464–3468, 2007.
[32] J. Xu, Q. Pan, and J. Qin, "Sensing characteristics of double layer film of ZnO," *Sens. Actuators B, Chem.*, vol. 66, no. 1, pp. 161–163, 2000.
[33] S. Kim, B. S. Kang, F. Ren, K. Ip, and Y. W. Heo, "Sensitivity of Pt/ZnO Schottky diode characteristics to hydrogen," *Appl. Phys. Lett.*, vol. 84, no. 10, pp. 1698–1700, 2004.
[34] H. Y. Lee, H. L. Huang, and C. T. Lee, "Hydrogen sensing performances of Pt/i-ZnO/GaN metal–insulator–semiconductor diodes," *Sens. Actuators B, Chem.*, vol. 157, no. 2, pp. 460–446, 2011.
[35] P. K. Basu, S. K. Jana, H. Saha, and S. Basu, "Low temperature methane sensing by electrochemically grown and surface modified ZnO thin films," *Sens. Actuators B, Chem.*, vol. 135, no. 1, pp. 81–88, 2008.
[36] S. N. Das, J. P. Kar, J. H. Choi, T. I. Lee, and K. J. Moon, "Fabrication and characterization of ZnO single nanowire-based hydrogen sensor," *J. Phys. Chem. C*, vol. 114, no. 3, pp. 1689–1693, 2010.
[37] J.-R. Huang, W.-C. Hsu, H.-I. Chen, and W.-C. Liu, "Comparative study of hydrogen sensing characteristics of a Pd/GaN Schottky diode in air and N 2 atmospheres," *Sens. Actuators B, Chem.*, vol. 123, no. 2, pp. 1040–1048, 2007.
[38] T. Hübert, L. Boon-Brett, G. Black, and U. Banach, "Hydrogen sensors—A review," *Sens. Actuators B, Chem.*, vol. 157, no. 2, pp. 329–352, 2011.
[39] A. Natan, L. Kronik, H. Haick, and R. T. Tung, "Electrostatic properties of ideal and non-ideal polar organic monolayers: Implications for electronic devices," *Adv. Mater.*, vol. 19, no. 23, pp. 4103–4117, 2007.
[40] A. Salehi, A. Nikfarjam, and D. J. Kalantari, "Pd/porous-GaAs Schottky contact for hydrogen sensing application," *Sens. Actuators B, Chem.*, vol. 113, pp. 419–427, 2006.
[41] M. R. Alenezi and A. S. Alshammari, "Role of the exposed polar facets in the performance of thermally and UV activated ZnO nanostructured gas sensors," *J. Phys. Chem. C*, vol. 117, no. 34, pp. 17850–17858, 2013.
[42] Z. Wang, J. Xue, D. Han, and F. Gu, "Controllable defect redistribution of ZnO Nanopyramids with exposed {1011} facets for enhanced gas sensing performance," *ACS Appl. Mater. Interfaces*, vol. 17, no. 1, pp. 17850–17858, 2014.

Lintu Rajan received the B.Tech. degree in electronics and communication engineering from Mahatma Gandhi University, Kerala, India, in 2009, and the M.Tech. degree in VLSI design from Amrita Vishwa Vidyapeetham University, Kerala, India, in 2011. She is currently working toward the Ph.D. degree in the Department of Electronics and Communication Engineering, Malaviya National Institute of Technology, Jaipur, India. Her research interest includes Electrical and Gas sensing characteristics of ZnO thin film-based schottky diodes.

C. Periasamy received the B.E. degree in electronics and communication engineering from Periyar University, Tamilnadu, India, in 2002, and the Ph.D. degree in electronics engineering from the Indian Institute of Technology, Banaras Hindu University, Varanasi, India, in 2011. He is currently working as an Assistant Professor in the Department of Electronics Engineering, Malaviya National Institute of Technology, Jaipur, India. His research interests include design, fabrication and characterization of nanomaterial-based electronic and piezoelectronic devices, thin film-based gas sensors, etc. He has published more than 35 papers in various international journals and conference proceedings.

Vineet Sahula received the Bachelor's degree in electronics (Hons.) from the Malaviya National Institute of Technology, Jaipur, India, in 1987, the Master's degree in integrated electronics and circuits from the Indian Institute of Technology (IIT) Delhi, New Delhi, India, in 1989, and the Ph.D. degree from the Department of Electrical Engineering, IIT Delhi, in 2001. He is currently the Professor of Department of Electronics and Communications Engineering, Malaviya National Institute of Technology, Jaipur, India. He has published more than 50 journals and conference papers to his credit. His current research interests include high-level design, modeling and synthesis for analog and digital systems, and computer-aided design for micro-electro-mechanical systems.

QUERIES

Q1. Author: Please provide the page range in Refs. [7], [17], and [23].

Comprehensive Study on Electrical and Hydrogen Gas Sensing Characteristics of Pt/ZnO Nanocrystalline Thin Film-Based Schottky Diodes Grown on N-Si Substrate Using RF Sputtering

Lintu Rajan, C. Periasamy, and Vineet Sahula, *Senior Member, IEEE*

***Abstract*—This paper presents a comprehensive study on the electrical characteristics of Pt/ZnO thin film Schottky contacts fabricated on n-Si substrates by RF sputtering, and its application as a Hydrogen sensor. The basic structural, surface morphological, and optical properties of the ZnO thin film were also been explored. Pt/ZnO thin film junction was characterized using current–voltage *(I–V)* and capacitance–voltage *(C–V)* measurements at room temperature, exhibiting rectifying behavior with barrier height, ideality factor and series resistance of 0.71 eV *(I–V)*/0.996 eV*(C–V),* 2.5 and ∼95 Ω respectively. The lack of congruence between the values of Schottky barrier heights calculated from *I–V* and *C–V* measurements is interpreted. Cheung's method and modified Norde's functions were employed along with the conventional thermionic emission model, to incorporate the impact of series resistance in the calculation of diode parameters. We unveiled, the Hydrogen sensing characteristics displayed by the Pt/ZnO thin film-based sensor to different concentrations (200–1000 ppm) of Hydrogen at 350 °C. The sensor has exhibited good recoverable transient characteristics under a series of Hydrogen exposure cycles with a maximum sensitivity of 57% at 1000 ppm of Hydrogen.**

***Index Terms*—Electrical characteristics, hydrogen sensing, metal-semiconductor interface, schottky diode, zinc oxide (ZnO) thin film.**

I. Introduction

INC Oxide have garnered widespread attention for the use in diverse applications such as gas sensors, lasers, solar cells, photo detectors, photo catalysts etc, owing to its distinctive properties such as good chemical and thermal stability, wide band gap (3.3 eV), high exciton binding energy (60 meV), high mobility of conducting electrons etc [1]–[6]. ZnO can form excellent Schottky or rectifying contact with high work function noble metals like Pt, Au and Pd and it is the one of the remarkable property due to which ZnO has attracted much research interest among solid state electronic researchers [1]–[10]. The rapid progress of ZnO devices like diodes, sensors, detectors, etc demand the proper understanding and controllability of its metal contacts.

Metal Schottky contact on ZnO was first studied by Mead and Neville [1]. Tsiarapas *et al.* and Yadav *et al.* investigated the Pd Schottky contact on ZnO and reported an ideality factor of ∼1.21 and ∼1.5 respectively [2], [3]. Aydogan *et al.* reported the electrical characterization of Au/n-ZnO Schottky contacts on n-Si using electro deposition technique with an ideality factor of ∼1.21 [4]. Periasamy and Chakrabarti also studied Pt contact on ZnO thin film using vacuum coating technique with an ideality factor of 1.52 [5]. Li *et al.* and Lp *et al.* reported the fabrication of Pt Schottky contacts on ZnO using pulse laser deposition with an ideality factor of ∼2.96 and ∼1.7 respectively [8], [11]. However, there is no significant report on fabrication and characterization of RF Sputtered Pt/ZnO Schottky contact on n-Si substrate for gas sensing applications.

Hydrogen has got heightened focus due to its importance in the present context where the shift to greener source of energy is highly demanding and Hydrogen can act as an alternative to fossil fuels. Extensive research in Hydrogen sensing is highly recommended as it is a colorless, odorless and highly inflammable gas which can spontaneously ignite with Oxygen forming potentially explosive mixtures [10]–[13]. Majority of commercial gas sensors are based on thin/thick layers or nanostructure-based metal oxide semiconductors, such as SnO_2,TiO_2, Fe_2O_3, ZnO, etc., integrated with heaters to raise the temperature to the achieve the optimum performance. ZnO nanostructure-based gas sensors simulated an exciting interest recently, due to their notable advantages, such as high surface to volume ratio, easy to fabricate structure, good chemical and thermal stability, better response, etc., [14]–[16]. Nanocrystalline thin films are having the additional advantage of reproducibility of film quality and ease of deposition. Also, it was reported that thin films possess better recovery characteristics compared to other configurations [17]. Noble metals like Pt, Pd and Au are considered to be important catalysts for Hydrogen sensing reactions [10].

We have investigated the Hydrogen sensing characteristics of Pt/ZnO thin film in this study. To the best of our knowledge, the proposed sensor structure, based on ZnO thin film with Pt catalytic dots on the surface, having the advantage of simple and easy to fabricate structure and devoid of any additional electrical contacts other than Pt catalytic contacts on the surface has not yet reported. We have discussed the trends in sensor performance and have tried to give an adequate explanation for

Manuscript received May 25, 2015; revised September 15, 2015 and December 17, 2015; accepted December 18, 2015. Date of publication; date of current version. This work was supported by CeNSE, Indian Institute of Science, Bangalore, where the part of the reported work (fabrication/characterization) was carried out under INUP which have been sponsored by DIT, MCIT, Government of India. The review of this paper was arranged by Associate Editor Z. Zhong.

The authors are with the Malaviya National Institute of Technology, Jaipur 302017, India (e-mail: linturajan08@gmail.com; cpsamy.ece@mnit.ac.in; vsahula.ece@mnit.ac.in).

Color versions of one or more of the figures in this paper are available online at http://ieeexplore.ieee.org.

Digital Object Identifier 10.1109/TNANO.2015.2513102

these trends. We have also discussed the basic microstructure study and optical properties of RF sputtered ZnO thin film.

II. Experimental Details

A. ZnO Thin Film Fabrication

ZnO thin film was deposited on the n-Si substrate (Resistivity of 1–10 Ω) by RF sputtering system equipped with high purity ZnO (99.99%) target. Before loading into the sputtering system, Si substrate of thickness 425 μm was organically and ionically cleaned using standard RCA process. The substrate was loaded into a magnetron sputtering system with a target to substrate distance fixed at 11 cm. Mechanical rotary and turbo pump were used to evacuate the sputtering chamber to the pressure of 1.5×10^{-6} Torr, before generation of plasma activated by RF power of 100 W. Sputtering gas used was Argon (99.999% pure) and its concentration was kept at 15 SCCM (standard cubic centimeter per minute) using the mass flow controller (MFC). To remove the impurities on ZnO target, it was pre-sputtered for 10 min before deposition. ZnO thin film was sputter deposited on substrates at the pressure of 1.8×10^{-2} Torr for 40 min. After deposition, rapid thermal annealing was performed at 450 °C for 10 min to improve the crystallinity of the film. The film thickness was measured by the surface profiler and was around 200 nm.

B. ZnO Thin Film Characterization

The crystalline properties of ZnO thin film were characterized by X-ray diffraction (XRD) using 18 kW Cu rotating-anode-based X-ray diffractometer (Panalytical X Pert Pro) with Cu Kα as the line source ($\lambda = 1.542$ Å). A Field emission scanning electron microscope (Nova Nano FE-SEM, 450) and Energy Dispersive X-ray (EDX) Spectroscopy (EDS-INCA, Oxford Instruments, UK) were used to investigate the surface morphologies and elemental compositions of the thin film respectively. Photoluminescence (PL) measurements at room temperatures were carried out using fluorescence spectrometer (Perkin Elmer, LS55) which uses a He–Cd laser of 325 nm emission line. Optical transmittance and absorbance of the film was measured using UV/VIS/NIS spectrometer (Perkin Elmer, Lambda 750), which uses deuterium and tungsten halogen light sources. All measurements were carried out at room temperature.

C. Device Fabrication and Characterization

To study the electrical properties and gas sensing behavior of ZnO thin film with Pt catalytic dots, an array of Pt Schottky contacts each of area 3.8×10^{-3} cm^2 and thickness 80 nm was fabricated on ZnO/n-Si substrate using RF sputtering through shadow mask technique. An 80 nm thick Al layer was also deposited on the back side of n-Si substrate by e-beam evaporation to obtain the ohmic contact. The fabricated device was then undergone rapid thermal annealing at 450 °C for 5 min to realize good electrical conductivity and better contact quality. The Fig. 1(a) shows the FE-SEM image (Top view) of Pt Schottky contacts arrays fabricated on the ZnO thin film, whereas the EDX spectrum is shown in Fig. 1(b). EDX spectrum exhibits an Oxygen peak at energy about 0.52 keV, two Zn peaks at 1.012 and 8.63 keV and two Pt peaks at 9.44 and 2.048 keV, confirming the presence of O, Zn and Pt elements respectively in our sample. The inset of Fig. 1(b) shows the elemental mapping of ZnO and Pt Schottky contacts in the sample. $I-V$ and $C-V$ measurements were obtained using Agilent B1500A semiconductor device analyzer. The gas sensing characteristics were obtained using a computer controlled gas sensing set up comprises of a static mixer, MFC, Keithley-237 source measure unit, a heater made of halogen bulb covered by graphite and a data acquisition system. The device was introduced to several gas exposure cycles of target gas of different concentrations and synthetic air at 350 °C.

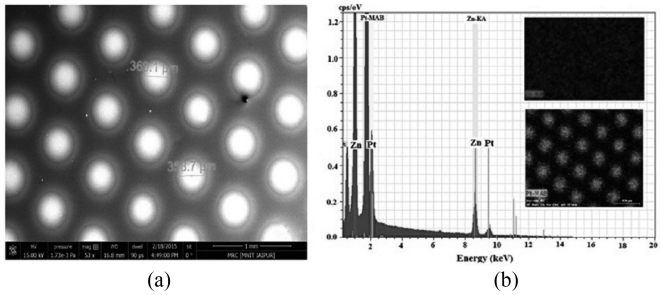

(a) (b)

Fig. 1. (a) FE-SEM image of Pt Schottky contacts grown on ZnO thin film. (b) EDX spectra of Pt/ZnO Schottky diodes, the inset shows the mapping data of ZnO (red) and Pt dots (green).

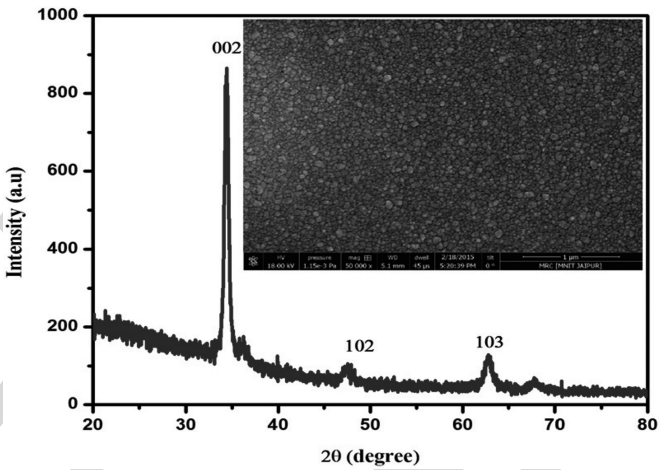

Fig. 2. The XRD pattern of ZnO thin film grown on Si substrate. Inset shows FE-SEM image of ZnO thin film.

III. Results and Discussions

A. Structural and Optical Properties of ZnO Thin Film

In Fig. 2 we present the XRD spectrum for the RF sputtered ZnO thin film on the silicon substrate in the range of 2θ from 20° to 80°. It is having highest peak of [002] appears at around $2\theta = 34.33°$ which is near to that of reference strain free ZnO film peak (34.421°) indicating good crystal quality of film with reduced stress. This also confirms that the film is preferentially C-axis oriented with hexagonal wurtzite structure. The Crystalline size (D) of ZnO thin film is calculated using the Scherrer formula from the full width at half maximum for the prominent

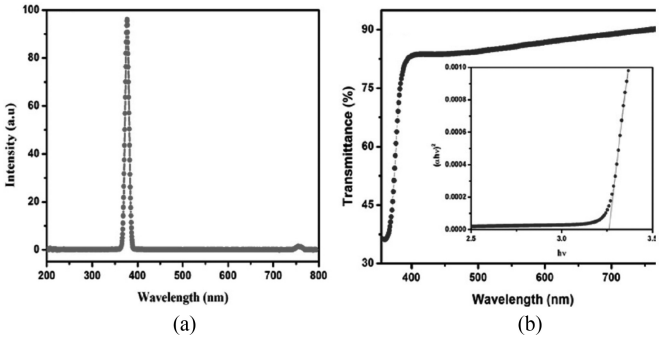

Fig. 3. (a) Room-temperature PL spectra of ZnO thin film on Si substrate. (b) Optical transmittance spectra of ZnO thin film as a function of wavelength. Inset shows the $(\alpha h\upsilon)^2$ versus $h\upsilon$ plot of ZnO thin film for band gap calculation.

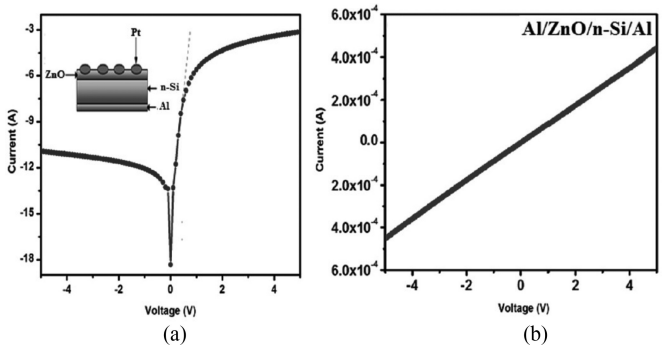

Fig. 4. (a) In *I–V* characteristic for Pt/ZnO thin film interface (dashed line represents linear fit). The inset shows *I–V* measurement set up. (b) The ohmic *I–V* characteristic of Al/n-ZnO/n-Si/Al junction.

(002) peak [18] and is around 18 nm. The lattice constant *c* and interplanar spacing *d* are evaluated to be 0.52033 and 0.2602 nm respectively. These values are in good accordance with the experimental results published by others [18], [19]. Inset of Fig. 2 depicts the FE-SEM image of the nanocrystalline ZnO thin film grown on n-Si substrate, which demonstrates that nanostructure grains are uniformly distributed having diameter of about 20 nm.

The PL characteristics of the ZnO thin films were procured in the wavelength range of 200–800 nm at room temperature and is depicted in Fig. 3(a). The film shows a strong UV emission peak at 375 nm which is known as near band edge emission, and it is attributed to the free exciton recombination. The absence of other major peaks, except UV emission confirms high crystallinity of the deposited ZnO thin films with fewer surface defects such as Oxygen vacancies [20]. The band gap of ZnO thin film is obtained as 3.28 eV from PL spectra.

The optical transmittance and absorbance of the film were measured by UV-Visible spectrometer in the range of 200–800 nm. Transmission spectra depicted in the Fig. 3(b) shows good optical transmission in the visible wavelength region (380–780 nm), confirming that sputtered ZnO thin film is transparent in the visible wavelength range. The optical band gap, for the film can be obtained by extrapolating the linear portions of $(\alpha h\upsilon)^2$ versus $h\upsilon$ to $\alpha h\upsilon = 0$, which is illustrated in the inset of Fig. 3(b) and its value is obtained as 3.26 eV [18]–[20].

B. I–V Characteristics of Pt/ZnO Thin Film Schottky Diode

The Pt/ZnO thin film Schottky diodes were electrically characterized using Agilent B1500A semiconductor device analyzer under dark condition. The fabricated Pt/ZnO/n-Si/Al structure is schematically represented in the inset of Fig. 4(a); whereas Fig. 4(a) shows the In *I–V* characteristics of the structure, which confirms the formation of Schottky junction at the Pt/ZnO interface having rectifying ratio I_F/I_R of 637 at ± 1 V. Since the Al/n-ZnO/Si/Al junction shows ohmic behavior as depicted in Fig. 4(b), the proposed structure behaves as vertical Pt/ZnO Schottky diode similar to structures reported by authors in [2]–[4], [21], [22]. We have measured *I–V* characteristics of about five Schottky diodes in the array. All of them exhibited the same characteristics. The Schottky diode parameters were extracted using three different techniques such as conventional thermionic emission model, Cheung's method and Norde's method, which are now discussed in detail. In the conventional method of calculation, we have extracted the electronic parameters such as saturation current, barrier height, and ideality factor of Pt/ZnO Schottky diode by assuming thermionic emission as the only carrier transport mechanism. The forward *I–V* characteristics of the Schottky junction is investigated with help of thermionic emission model, in which current for positive bias voltage is given by (1),neglecting the series resistance [21]–[26].

$$I \approx I_0 \left[\exp\left(\frac{qV}{\eta kT}\right) - 1\right] \tag{1}$$

where, I_0 is the saturation current as depicted in (2), q is the electronic charge, V is the applied voltage, η is the ideality factor, k is the Boltzmann constant and T is the temperature.

$$I_0 = AA^*T^2 \exp\left(\frac{-q\phi_b}{kT}\right) \tag{2}$$

where A is the diode area, $A^*(= 32\,\mathrm{cm}^{-2}\,\mathrm{K}^{-2})$ is the Richardson constant, ϕ_b is the effective barrier height at zero bias [1], [3], [5]. We have calculated the slope of low voltage linear region (0.1 V to 0.3 V) of forward bias In *I–V* characteristics and obtained the value of ideality factor as 2.5 at room temperature using (3) [1], [3], [5].

$$\eta = \frac{q}{kT}\frac{dV}{d\ln(I)}. \tag{3}$$

The departure of ideality factor from the ideal value of 1 indicates the existence of different current conduction mechanisms other than thermionic emission in the Schottky junction like tunneling, tunneling-recombination, field emission etc, presence of series resistance and interfacial layer between metal and semiconductor [23], [27]. The saturation current is calculated from the vertical axis intercept of In *I–V* plot and obtained to be 1.5×10^{-8} A. Effective Barrier height of the Schottky junction is calculated to be 0.71 eV using (2).

These values are in good congruence with the results published by other researchers [5], [8]. According to Schottky–Mott theory, the ideal value of the barrier height for Pt/ZnO Schottky contact varies from 1.3 to 1.95 eV which is given by the difference between work function of Pt and electron affinity of ZnO [23]. The non-ideal values of barrier height (0.71 eV)

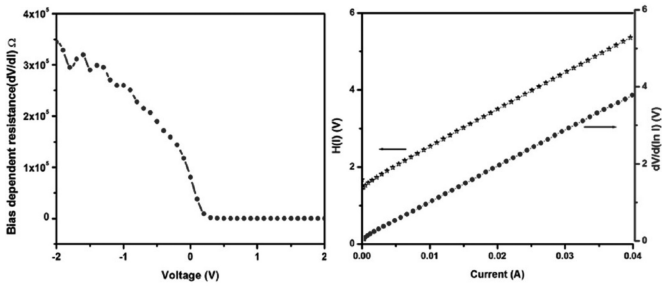

Fig. 5. (a) Bias voltage dependent diode resistance (R_i) of Pt/ZnO interface. (b) Plots of $dv/d(\ln I)$ versus I and $H(I) - I$ of Pt/ZnO thin film diode obtained from experimental *I–V* data in Fig. 4(a).

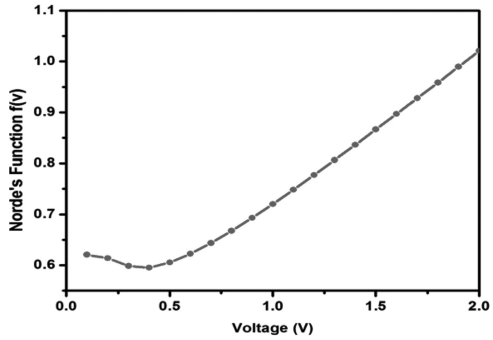

Fig. 6. $F(V)$ versus V plots obtained from the experimental *I–V* data in Fig. 4(a).

and ideality factor (2.5) measured from *I–V* characteristic can be credited to the presence of interface states between metal (Pt) electrode and semiconductor (ZnO) surface, Fermi energy level pinning caused by surface states, barrier inhomogeneities and certain other interface specific effects [1], [2], [23], [27].

In order to gain insight regarding the value of series resistance, we studied bias dependent resistance, $R_i (R_i = dV/dI)$ *versus* V plot as shown in Fig. 5(a). It is obvious from the plot that that R_i has got a bias independent constant value of around 95 Ω at higher voltages, and this corresponds to series resistance [22]. To incorporate the effect of series resistance, R_s in our Schottky diode parameter calculations, we have employed the analysis technique reported by Cheung and Cheung [28]. Cheung's functions can be written as:

$$\frac{dV}{d(\ln I)} = \frac{\eta kT}{q} + IR_s \tag{4}$$

$$H(I) = V - \frac{\eta kT}{q} \ln\left(\frac{I}{AA^*T^2}\right) \tag{5}$$

$$H(I) = \eta\phi_b + IR_s. \tag{6}$$

From the slope and vertical axis intercept of $dv/d(\ln I)$ versus I plot displayed in Fig. 5(b), value of series resistance (R_s) and ideality factor η are obtained as 96.2 Ω and 2.34 respectively. In order to determine the value of barrier height, we have also plotted $H(I)$ versus I curve using the value of ideality factor obtained from $dv/d(\ln I)$ versus I plot. Schottky barrier height (ϕ_b) is extracted from the vertical axis intercept of *H(I)* versus *I* plot given in the Fig. 5(b) and is obtained as 0.65 eV, whereas its slope will give the value of series resistance, which is equal to 96.6 Ω. There is a disparity in the Schottky barrier height value obtained from conventional thermionic emission model and Cheung's technique. This is because, Cheung's plots are obtained from the downward curvature region of *I–V* characterization, which strongly suggests the presence of series resistance and insulating interfacial layer across Pt/ZnO Schottky junction, whereas parameters are calculated from low voltage linear region of *I–V* characteristic in thermionic emission model. Furthermore, the closely agreed values of series resistance calculated from both the plots of Fig. 5(b), is a proof for the consistency of Cheung's approach of calculations [2], [4], [28]. An alternative approach developed by Norde is also employed to determine the value of series resistance [29], [30]. The Norde function is described as in (7).

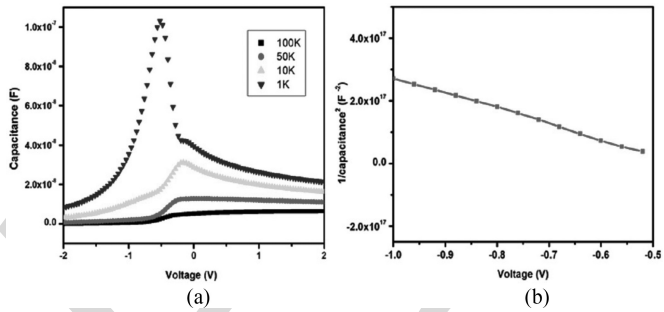

Fig. 7. (a) The frequency dependent *C–V* characteristics of Pt/ZnO Schottky diode. (b) $C^{-2} - V$ characteristics of Pt/ZnO Schottky diode at $f = 50$ KHz.

$$F(V) = \frac{V}{\gamma} - \frac{kT}{q} \ln\left(\frac{I(V)}{AA^*T^2}\right) \tag{7}$$

$$\phi_b = F(V_{\min}) + \frac{V_o}{\gamma} - \frac{kT}{q} \tag{8}$$

$$R_s = \frac{kT(\gamma - n)}{qI} \tag{9}$$

where γ is an integer greater than ideality factor (here 3), $I(V)$ is the current obtained from *I–V* curve, $F(V_{\min})$ is the minimum value of $F(V)$ and V_0 is the voltage corresponding to $F(V_{\min})$. Fig. 6 depicts the $F(V)$ versus V curve of the Pt/ZnO thin film Schottky diode. The value of barrier height and series resistance obtained from Norde's technique using (8) and (9) are 62.5 Ω and 0.73 eV respectively. These values are in near accordance with value that obtained from the conventional thermionic emission model and Cheung's method, confirming the accuracy of our calculations.

C. C–V Characteristics of Pt/ZnO Thin Film Schottky Diode

Fig. 7(a) displays the frequency dependence of *C–V* characteristics of Pt/ZnO thin film Schottky diode. The graph illustrates that capacitance decreases with increasing frequency, which is an evidence for the existence of interface states and its progressive decrease of the response to the applied ac voltage [27]. At lower frequencies, the interface states can faith-

fully follow the ac signal resulting in higher capacitance values; whereas at higher frequencies, contribution of interface states to total capacitance is very small resulting in lower capacitance value, since the charge at interface states cannot respond spontaneously to the ac signal, [29]–[31]. The *C–V* characteristics can be studied with the help of reverse bias $C^{-2} - V$ characteristics of the diode depicted in Fig. 7(b). The linear curve confirms that doping concentration N_d is constant throughout the depletion region. Depletion layer capacitance is given by following equations.

$$\frac{1}{C^2} = \frac{2\left(V_{\rm bi} - V - \frac{kT}{q}\right)}{q\varepsilon_s\varepsilon_0 A^2 N_d} \tag{10}$$

$$\frac{d(C^{-2})}{d(V)} = \frac{2}{q\varepsilon_s\varepsilon_0 A^2 N_d} \tag{11}$$

where, $V_{\rm bi}$ is the built-in potential, obtained from the intercept of $C^{-2} - V$ curve, ε_s the dielectric constant of the semiconductor ($9\varepsilon_0$ for ZnO), ε_0 is the dielectric constant of vacuum ($8.85 \times 10^{-12}\,\mathrm{F/m}$), N_d is the concentration of ionized donors and A is the diode area [27], [29].

Carrier concentration N_d can be determined from the slope of $C^{-2} - V$ curve, using (11) and found to be $1 \times 10^{16}\,\mathrm{cm}^{-3}$. The barrier height of Pt/ZnOSchottky contact can be obtained from *C–V* measurements using (12).

$$\phi_b = q\left[V_{\rm bi} + \frac{kT}{q}\ln\frac{N_c}{N_d}\right] \tag{12}$$

where, N_c is the density of states in the conduction band and its value is $3.5 \times 10^{18}\,\mathrm{cm}^{-3}$ for ZnO at room temperature [22]. The barrier height of Pt/ZnO thin film Schottky diode is determined as 0.996 eV from the *C–V* measurement which is larger than the barrier heights obtained from the *I–V* measurements. This barrier height variation is possibly due to the effect of lowering of barrier energy induced by image force for (Schottky effect), barrier in-homogeneities caused by intrinsic and extrinsic factors such as grain boundaries, defects, etc., metal induced gap states and presence of an unavoidable interface layer between metal and semiconductor surface [26].

The density of interface states, $N_{\rm ss}$ was calculated using *I–V* and *C–V* characteristics using (13) [22], [28]–[30].

$$N_{\rm ss} = \frac{1}{q}\left[\frac{\varepsilon_i}{\delta}\{n(V) - 1\} - \frac{\varepsilon_s}{W_D}\right] \tag{13}$$

where, ε_i is the permittivity of interface layer, δ is the interface layer thickness, $n(V)$ is the voltage dependent ideality factor and W_D is the width of depletion layer which was obtained from *C–V* characteristics. The value of $N_{\rm ss}$ was obtained to be around $2.03 \times 10^{15}\,\mathrm{eV}^{-1}\mathrm{cm}^{-2}$ at 0.5 V.

D. Gas Sensing Properties of Pt/ZnO Thin film

In the proposed sensor structure, the sensor element, i.e., nanocrystalline ZnO thin film is provided with Pt catalytic dots or Schottky contacts on the surface. We represent the *I–V* characteristics of the sensor at different Hydrogen concentrations and air in Fig. 8, whereas its inset provides the schematic structure of the sensor. We have also studied the Hydrogen sensing

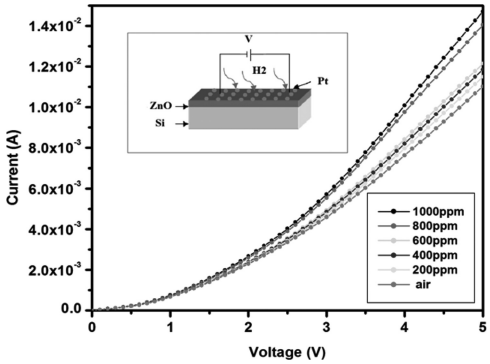

Fig. 8. *I–V* characteristics of the sensor at different Hydrogen concentrations at 350 °C., Inset shows schematic structure of proposed sensor.

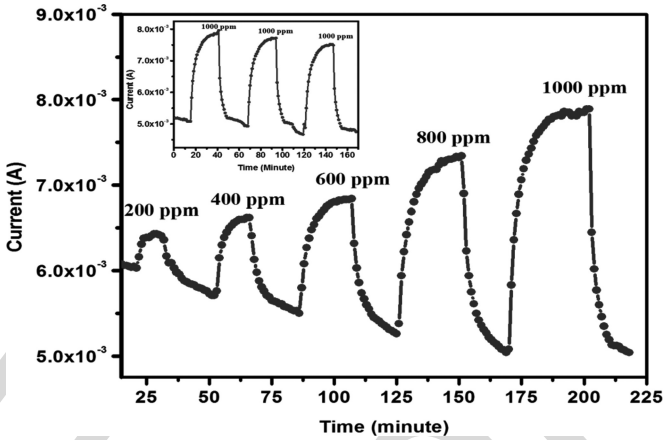

Fig. 9. Dynamic characteristic of the device at different concentrations of Hydrogen at 350 °C. Inset shows repeatability of device at 1000 ppm Hydrogen and 350 °C.

capability of the device by monitoring the current change caused by the adsorption and desorption of target gas (H_2) at 200 ppm-1000 ppm of Hydrogen at 350 °C. which is represented in Fig. 9 and its inset elucidate the repeatability of device at the 1000 ppm Hydrogen. The Sensitivity of the device, *S* was defined as the relative variation of the current in the presence and absence of Hydrogen and is given by (14) [25], [26].

$$S(\%) = \left\{\frac{I_{H_2} - I_{\rm air}}{I_{\rm air}}\right\} \times 100 \tag{14}$$

where, $I_{\rm air}$ is sensor current in the presence of air and I_{H2} is the sensor current after exposing to H_2 gas. The sensitivity has been calculated using (14), and it is noted that sensitivity is directly proportional to Hydrogen concentration, having values of 6.46%, 15.7%, 23.9%, 39.8% and 57% at Hydrogen concentrations of 200 ppm, 400, 600, 800 and 1000 ppm respectively. We have observed a considerable drift in the baseline current of the sensor at different concentrations, which is explained in the later section. Response time of our sample is calculated as the time required for the sensor current to reach 90% of the saturation value in the presence of Hydrogen whereas recovery time is defined as the time required for the sensor current to return to 10% of its baseline value in the presence of synthetic air. It would be worth noting that, while response time increases with increase

TABLE I
ELECTRICAL AND GAS SENSING PARAMETERS OF PT/ZNO THIN FILM SCHOTTKY DIODE

A	Electrical characteristics of Pt/ZnO thin film Schottky diode			
		Cheung's method		
Parameters	Conventional *I-V* method	dV/dlnI versus I	H(I) versus I	Norde's method
Ideality factor	2.5	2.34	–	–
Barrier height (eV)	0.71	0.65	–	0.73
Series resistance (Ω)	∼95	96.2	96.6	62.5

B	Gas sensing characteristics of Pt/ZnO thin film Schottky diode				
	Concentration of Hydrogen				
Parameter	200	400	600	800	1000
Sensitivity (%)	6.46	15.7	23.9	39.8	57
Response(min)	2	5	6	11	15
Recovery(min)	2	4	4	3.5	3.5

in Hydrogen concentration, there is no significant change in recovery time as the target gas concentration increases. It is interesting to note that, in this study recovery time is less than the response time, and similar to observation as reported by Hassan *et al.* [26]. All the sensing parameters obtained from are listed in Table I. We have analyzed the possible reasons for the various trends observed in sensor performance and proposed justification for these trends in the following section.

A brief review on previously reported literature on the Hydrogen sensing characteristics of ZnO, incorporating Pt as the catalyst has been provided in Table II [17], [32]–[34]

E. Hydrogen Sensing Mechanism of Pt/ZnO Thin Film

The change in electrical conductivity of the sensor element upon introduction and removal of target gas can be explained as follows: when Pt/ZnO thin film junction is exposed to synthetic air, Oxygen molecules will get chemisorbed on ZnO surface, forming Oxygen ions by extracting electrons from the conduction band of ZnO. This will create a depletion region in the ZnO surface, causing high electrostatic potential across Pt/ZnO Schottky interface and decreasing the electrical conductivity of ZnO surface. The Pt dots on ZnO thin film can enhance the Oxygen spill over process, by providing a lower energy path for the gaseous species be adsorbed on the metal surface and then diffuse to the ZnO surface [35], [36]. This can result in a large amount of chemisorbed Oxygen. Oxygen chemisorptions reactions are represented as $\mathrm{O}_{2(\mathrm{gas})+}e- \rightarrow \mathrm{O}^{-}_{2(\mathrm{ads}),}\mathrm{O}^{-}_{2(\mathrm{ads})} + \mathrm{e} \rightarrow 2\mathrm{O}^{-}_{(\mathrm{ads}),}2\mathrm{O}^{-}_{(\mathrm{ads})} + \mathrm{e} \rightarrow \mathrm{O}^{2^{-}}_{(\mathrm{ads})}$ [24].

It is important to note that noble metals like Pt, Pd and Au on metal oxide surface can act as a catalyst for dissociation of Hydrogen into Hydrogen atoms [10], [37], [38]. The hydrogen atoms then diffuse through the Pt to reach Pt/ZnO interface and the built-in electric field causes the polarization of Hydrogen atoms, resulting in a dipole layer at Pt/ZnO interface, which will lowers the work function of metal and the Schottky barrier height, increasing the current flow [10], [39]. This is obvious from the *I–V* characteristics of the sensor in Fig. 8. The increase in electrical conductivity of sensor element upon exposure to Hydrogen can also be attributed to the surface reaction between dissociated Hydrogen atoms and chemisorbed Oxygen species on ZnO thin film surface and the subsequent release of electrons to the conduction band of ZnO. The chemical reactions involved are reproduced below $4\mathrm{H} + \mathrm{O}_2^- \rightarrow 2\mathrm{H}_2\mathrm{O} + \mathrm{e}^-$, $2\mathrm{H} + \mathrm{O} \rightarrow \mathrm{H}_2\mathrm{O} + \mathrm{e}^-$, $2\mathrm{H} + \mathrm{O}^2 \rightarrow \mathrm{H}_2\mathrm{O} + 2\mathrm{e}^-$ [25], [36].

In transient response curves given in Fig. 9, we observe a major drift in the baseline current value in the repeated exposure cycles of Hydrogen and synthetic air. This can be attributed to the inefficient chemisorptions of Oxygen molecules and incomplete desorption of Hydrogen atoms from ZnO thin film surface upon exposure to synthetic air [26]. It is also reported that noble metals like Pd and Pt undergo volume change upon repeated Hydrogen exposure, causing embrittlement effect and adversely affect the stability of sensor [38], [39]. However, high temperature enhances the desorption rate which is evidenced from the small recovery time. It is clear from Table I, that the response time increases with the increase in concentration of Hydrogen in the subsequent cycles. This can be attributed to the additional hydroxyl and water products formation during Hydrogen adsorption process. This event could also be the reason for the instability of baseline current value [37], [40].

The sensitivity, S as a function of Hydrogen concentration can empirically be expressed as in (15) [24], [41].

$$S = A(C_{(g)})^{\beta} + 1 \tag{15}$$

where *A* and β are empirically obtained parameters depends on the stoichiometry of surface reactions involved in gas sensing, C_g is the target gas concentration. It was reported that β is 0.5, if the adsorbed Oxygen species is O^{2-} and is 1 if the dominant adsorbed species is O^- [24], [35]. The equation in (15) can also be expressed as follows.

$$\log(S_g - 1) = \log A + \beta \log C_{(g)}. \tag{16}$$

The Fig. 10 depicts the plot of $\log(S_g - 1)$ versus $\log C_{\mathrm{g}}$ which is linear according to (16) with a slope of $\beta = 0.95$. The value of β strongly recommends that the dominant adsorbed Oxygen species on the ZnO thin film surface is O^-. It is worth mentioning that doubly negative Oxygen ion (O^{2-}) is more efficient in depleting the ZnO surface and thus enhancing the sensitivity of Pt/ZnOSchottky junction compared to O^- [41].

TABLE II
A BRIEF SUMMARY OF ZNO BASED HYDROGEN SENSORS, INCORPORATING PT AS A CATALYST

Sensing Material	Deposition Technique	Concentration of Hydrogen	Sensing Performance	Ref
Pt-doped ZnO single layer film	Chemical precipitation	0.2%	$\sim$2 (R_{air}/R_{H2}) (330 °C)	[32]
Pt/ZnO Schottky diode	E-Beam Evaporation	5 ppm H_2	Change of 50 mV bias at 8 mA.(298 K)	[33]
Pt/iZnO Schottky diode	CVD	10 000 ppm	Barrier height change = 207.8 mV(350 K)	[34]
Pt-coated ZnO thin film/Nanorod	PLD(thin film), MBE(Nanorod)	500 ppm	Response of nanorod is higher	[17]
ZnO thin film with Pt dots(*Current work*)	RF sputtering	1000 ppm	Relative Response of 57% (350 °C)	–

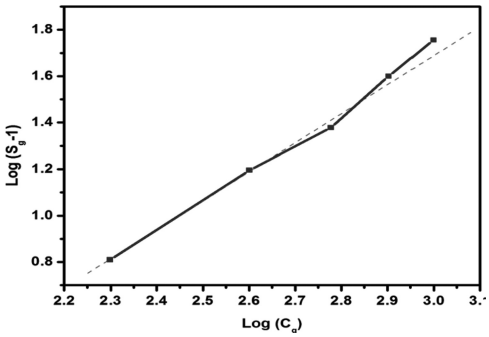

Fig. 10. $\log(S_g - 1)$ versus *log* C_g plot of Pt/ZnO thin film based Hydrogen sensor (dashed line represents the linear fit).

The less abundance of O^- on the Pt/ZnO thin film surface could be a reason for the relatively low sensitivity of the proposed device at the lower concentrations of Hydrogen.

The PL spectra of ZnO thin film elucidated in Fig. 3(a) is devoid of any broad emission peaks except the major emission peak at 380 nm which confirms that the ZnO thin film is highly crystalline with minimum surface defects such as Oxygen vacancies (V_0^{2+}). It is reported that defects such as Oxygen vacancies can enhance the adsorption and desorption process on the ZnO surface by making the nanostructure unstable and increasing the adsorption sites on film surface [24]. Thus, the minimum number of defects on ZnO thin film surface could justify for higher response time of Pt/ZnO thin film surface at higher concentrations.

We have obtained the optimum results at high temperature (350 °C). Many reports have also confirmed this fact that, a nanostructured ZnO-based gas sensors exhibits maximum sensitivity at elevated temperatures usually above 300 °C. This could be attributed to the fact that, Hydrogen atoms can overcome the potential barrier to react with adsorbed Oxygen species only at high temperatures [36], [41]. It is worth mentioning that the factors such as surface to volume ratio, surface defects, quantity of adsorption sites, etc., have significant impact on the surface-controlled reactions involved in gas sensing mechanism of metal oxide semiconductor-based gas sensors. The performance of Pt/ZnO thin film junction can be further improved by optimizing the surface morphology of sensor surface [40]–[42].

IV. CONCLUSION

In this manuscript, we have investigated the electrical and gas sensing characteristics of Pt/ZnOthin film Schottky contacts grown on n-Si substrate by RF sputtering. The structural and optical properties of the ZnO thin film have been characterized by XRD, FE-SEM, EDX, UV and PL spectroscopy, which has confirmed its good crystalline nature. We have estimated characteristic parameters of Pt/ZnOSchottky diode such as barrier height, ideality factor and series resistance, using (*I–V*) and (*C–V*) characterizations being $\sim$0.71 eV $(I - V)/\sim 0.996\,\mathrm{eV}$ (*C–V*), $\sim$2.25 and $\sim$95 Ω respectively at room temperature. An investigation on the gas sensing characteristics of the device towards different concentrations of Hydrogen (200–1000 ppm) at 350 °C revealed a maximum sensitivity of 57% at 1000 ppm Hydrogen. The device has been proposed to be of simple and easy to fabricate structure, having response increasing linearly with Hydrogen concentration.

ACKNOWLEDGMENT

The authors would like to thanks Materials Research Centre, MNIT Jaipur for the fabrication and characterization facility.

REFERENCES

[1] R. C. Neville and C. A. Mead, "Surface barriers on zinc oxide," *J. Appl. Phys.*, vol. 41, no. 9, pp. 3795–3800, 1970.
[2] C. Tsiarapas, D. Girginoudi, and N. Georgoulas, "Electrical characteristics of Pd Schottky contacts on ZnO films," *Mater. Sci. Semicond. Process.*, vol. 17, pp. 199–206, 2014.
[3] A. B. Yadav, A. Pandey, and S. Jit, "Pd Schottky contacts on sol-gel derived ZnO thin films with nearly ideal richardson constant," *IEEE Electron Device Lett.*, vol. 35, no. 7, pp. 729–731, Jul. 2014.
[4] S. Aydogan, K. Cinar, H. Asil, C. Coskun, and A. Turut, "Electrical characterization of Au/n-ZnO Schottky contacts on n-Si," *J. Alloys Compounds*, vol. 476, no. 1, pp. 913–918, 2009.
[5] C. Periasamy and P. Chakrabarti, "Structural and electrical properties of metal contacts on n-type ZnO thin film deposited by vacuum coating technique," *J. Vac. Sci. Technol. B*, vol. 27, no. 5, pp. 2124–2127, Aug. 2009.
[6] J. Iqbal, T. Jan, Y. Ronghai, S. H. Naqvi, and I. Ahmad, "Doping induced tailoring in the morphology, band-gap and ferromagnetic properties of biocompatible ZnO nanowires, nanorods and nanoparticles," *Micro Nano Lett.*, vol. 6, no. 3, pp. 242–251, 2014.
[7] C. Periasamy and P. Chakrabarti, "Time-dependent degradation of Pt/ZnO nanoneedle rectifying contact based piezoelectric nanogenerator," *J. Appl. Phys.*, vol. 109, p. 054306, 2011.
[8] Y. Z. Li, X. M. Li, and X. D. Gao, "Effects of post-annealing on Schottky contacts of Pt/ZnO films toward UV photodetector," *J. Alloys Compounds*, vol. 509, no. 26, pp. 7193–7197, 2011.
[9] Z. Shao, L. Wen, D. Wu, X. Zhang, S. Chang, and S. Qin, "Pt/ZnO Schottky nano-contact for piezoelectric nanogenerator," *Phys. E, Low Dimensional Syst. Nanostruct.*, vol. 43, no. 1, pp. 173–175, 2010.
[10] A. B. Yadav, C. Periasamy, S. Bhaumik, and S. Jit, "Hydrogen gas sensing properties of Pd/ZnO thin films grown on n-Si substrates at room-temperature by thermal evaporation and sol-gel techniques: A comparative study," *Indian J. Pure Appl. Phys.*, vol. 51, no. 11, pp. 792–799, 2013.
[11] K. Ip, Y. W. Heo, K. H. Baik, D. P. Norton, S. J. Pearton, S. Kim, J. R. LaRoche, and F. Ren, "Temperature-dependent characteristics of Pt Schottky contacts on n -type ZnO," *Appl. Phys. Lett.*, vol. 84, no. 15, pp. 2835–2837, 2004.

[12] D. Kohl, "Function and applications of gas sensors," *J. Phys. D, Appl. Phys.*, vol. 34, no. 19, pp. R 125–R 149, 2001.
[13] J. Graetz, "New approaches to hydrogen storage," *Chem. Soc. Rev.*, vol. 38, no. 1, pp. 73–82, 2009.
[14] E. Comini, C. Baratto, I. Concina, and G. Faglia, "Metal oxide nanoscience and nanotechnology for chemical sensors," *Sens. Actuators B, Chem.*, vol. 179, pp. 3–20, 2013.
[15] P. T. Moseley, "Materials selection for semiconductor gas sensors," *Sens. Actuators B, Chem.*, vol. 6, no. 1, pp. 149–156, 1992.
[16] J. Wang, F. Yang, X. Wei, Y. Zhang, and L. Wei, "Controlled growth of conical nickel oxide nanocrystals and their high performance gas sensing devices for ammonia molecule detection," *Phys. Chem. Chem. Phys.*, vol. 16, no. 31, pp. 16711–16718, 2014.
[17] L. C. Tien, P. W. Sadik, D. P. Norton, and L. F. Voss, "Hydrogen sensing at room temperature with Pt-coated ZnO thin films and nanorods," *Appl. Phys. Lett.*, vol. 87, no. 22, p. 222106, 2005.
[18] S. Sharma, S. Vyas, C. Periasamy, and P. Chakrabarti, "Structural and optical characterization of ZnO thin films for optoelectronic device applications by RF sputtering technique," *Superlattices Microstruct.*, vol. 75, pp. 378–389, 2014.
[19] C. Gu, J. Li, J. Lian, and G. Zheng, "Electrochemical synthesis and optical properties of ZnO thin film on In 2 O 3: Sn (ITO)-coated glass," *Appl. Surf. Sci.*, vol. 253, no. 17, pp. 7011–7015, 2007.
[20] P.-T. Hsieh, Y.-C. Chen, C.-M. Wang, Y.-Z. Tsai, and C.-C. Hu, "Structural and photoluminescence characteristics of ZnO films by room temperature sputtering and rapid thermal annealing process," *Appl. Phys. A*, vol. 84, pp. 345–349, 2006.
[21] D. Somvanshi and S. Jit, "Mean barrier height and Richardson constant for Pd/ZnO thin film-based Schottky diodes grown on n-Si substrates by thermal evaporation method," *IEEE Electron. Device Lett.*, vol. 34, no. 10, pp. 1238–1240, Oct. 2013.
[22] D. Somvanshi and S. Jit, "Analysis of I–V characteristics of Pd/ZnO thin film/n-Si schottky diodes with series resistance," *J. Nanoelectron. Optoelectron.*, vol. 9, pp. 21–26, 2014.
[23] I. Hussain, M. Y. Soomro, N. Bano, O. Nur, and M. Willander, "Interface trap characterization and electrical properties of Au-ZnO nanorod Schottky diodes by conductance and capacitance methods," *J. Appl. Phys.*, vol. 112, no. 6, p. 064506, 2012.
[24] Y. Shi, M. Wang, C. Hong, Z. Yang, J. Deng, and X. Song, "Multi-junction joints network self-assembled with converging ZnO nanowires as multi-barrier gas sensor," *Sens. Actuators B, Chem.*, vol. 177, pp. 1027–1034, 2013.
[25] S. Ren, G. Fan, S. Qu, and Q. Wang, "Enhanced H2 sensitivity at room temperature of ZnO nanowires functionalized by Pd nanoparticles," *J. Appl. Phys.*, vol. 110, p. 084312, 2011.
[26] J. J. Hassan, M. A. Mahdi, C. W. Chin, and H. Abu-Hassan, "A high-sensitivity room-temperature hydrogen gas sensor based on oblique and vertical ZnO nanorod arrays," *Sens. Actuators B, Chem.*, vol. 176, pp. 360–367, 2013.
[27] S. M. Sze, *Physics of Semiconductor Devices*, 2nd ed. New York, NY, USA: Wiley, 1981.
[28] S. K. Cheung and N. W. Cheung, "Extraction of Schottky diode parameters from forward current-voltage characteristics," *Appl. Phys. Lett.*, vol. 49, no. 2, pp. 85–87, 1986.
[29] S. Karataş, S. Altındal, A. Türüt, and M. Cakar, "Electrical transport characteristics of Sn/p-Si schottky contacts revealed from I–V–T and C–V–T measurements," *Phys. B, Condens. Matter*, vol. 392, nos. 1/2, pp. 43–50, 2007.
[30] W. G. Osiris, A. A. M. Farag, and I. S. Yahia, "Extraction of the device parameters of Al/P 3 OT/ITO organic Schottky diode using J–V and C–V characteristics," *Synthetic Metals*, vol. 161, no. 11, pp. 1079–1087, 2011.
[31] M. Cakar, N. Yıldırım, H. Doğan, and A. Türüt, "The conductance and capacitance–frequency characteristics of Au/pyronine-B/p-type Si/Al contacts," *Appl. Surf. Sci.*, vol. 253, pp. 3464–3468, 2007.
[32] J. Xu, Q. Pan, and J. Qin, "Sensing characteristics of double layer film of ZnO," *Sens. Actuators B, Chem.*, vol. 66, no. 1, pp. 161–163, 2000.
[33] S. Kim, B. S. Kang, F. Ren, K. Ip, and Y. W. Heo, "Sensitivity of Pt/ZnO Schottky diode characteristics to hydrogen," *Appl. Phys. Lett.*, vol. 84, no. 10, pp. 1698–1700, 2004.
[34] H. Y. Lee, H. L. Huang, and C. T. Lee, "Hydrogen sensing performances of Pt/i-ZnO/GaN metal–insulator–semiconductor diodes," *Sens. Actuators B, Chem.*, vol. 157, no. 2, pp. 460–446, 2011.
[35] P. K. Basu, S. K. Jana, H. Saha, and S. Basu, "Low temperature methane sensing by electrochemically grown and surface modified ZnO thin films," *Sens. Actuators B, Chem.*, vol. 135, no. 1, pp. 81–88, 2008.
[36] S. N. Das, J. P. Kar, J. H. Choi, T. I. Lee, and K. J. Moon, "Fabrication and characterization of ZnO single nanowire-based hydrogen sensor," *J. Phys. Chem. C*, vol. 114, no. 3, pp. 1689–1693, 2010.
[37] J.-R. Huang, W.-C. Hsu, H.-I. Chen, and W.-C. Liu, "Comparative study of hydrogen sensing characteristics of a Pd/GaN Schottky diode in air and N 2 atmospheres," *Sens. Actuators B, Chem.*, vol. 123, no. 2, pp. 1040–1048, 2007.
[38] T. Hübert, L. Boon-Brett, G. Black, and U. Banach, "Hydrogen sensors—A review," *Sens. Actuators B, Chem.*, vol. 157, no. 2, pp. 329–352, 2011.
[39] A. Natan, L. Kronik, H. Haick, and R. T. Tung, "Electrostatic properties of ideal and non-ideal polar organic monolayers: Implications for electronic devices," *Adv. Mater.*, vol. 19, no. 23, pp. 4103–4117, 2007.
[40] A. Salehi, A. Nikfarjam, and D. J. Kalantari, "Pd/porous-GaAs Schottky contact for hydrogen sensing application," *Sens. Actuators B, Chem.*, vol. 113, pp. 419–427, 2006.
[41] M. R. Alenezi and A. S. Alshammari, "Role of the exposed polar facets in the performance of thermally and UV activated ZnO nanostructured gas sensors," *J. Phys. Chem. C*, vol. 117, no. 34, pp. 17850–17858, 2013.
[42] Z. Wang, J. Xue, D. Han, and F. Gu, "Controllable defect redistribution of ZnO Nanopyramids with exposed {1011} facets for enhanced gas sensing performance," *ACS Appl. Mater. Interfaces*, vol. 17, no. 1, pp. 17850–17858, 2014.

Lintu Rajan received the B.Tech. degree in electronics and communication engineering from Mahatma Gandhi University, Kerala, India, in 2009, and the M.Tech. degree in VLSI design from Amrita Vishwa Vidyapeetham University, Kerala, India, in 2011. She is currently working toward the Ph.D. degree in the Department of Electronics and Communication Engineering, Malaviya National Institute of Technology, Jaipur, India. Her research interest includes Electrical and Gas sensing characteristics of ZnO thin film-based schottky diodes.

C. Periasamy received the B.E. degree in electronics and communication engineering from Periyar University, Tamilnadu, India, in 2002, and the Ph.D. degree in electronics engineering from the Indian Institute of Technology, Banaras Hindu University, Varanasi, India, in 2011. He is currently working as an Assistant Professor in the Department of Electronics Engineering, Malaviya National Institute of Technology, Jaipur, India. His research interests include design, fabrication and characterization of nanomaterial-based electronic and piezoelectronic devices, thin film-based gas sensors, etc. He has published more than 35 papers in various international journals and conference proceedings.

Vineet Sahula received the Bachelor's degree in electronics (Hons.) from the Malaviya National Institute of Technology, Jaipur, India, in 1987, the Master's degree in integrated electronics and circuits from the Indian Institute of Technology (IIT) Delhi, New Delhi, India, in 1989, and the Ph.D. degree from the Department of Electrical Engineering, IIT Delhi, in 2001. He is currently the Professor of Department of Electronics and Communications Engineering, Malaviya National Institute of Technology, Jaipur, India. He has published more than 50 journals and conference papers to his credit. His current research interests include high-level design, modeling and synthesis for analog and digital systems, and computer-aided design for micro-electro-mechanical systems.

QUERIES

Q1. Author: Please provide the page range in Refs. [7], [17], and [23].